

Lobitz

SAND78-0962
Unlimited Release

ECONOMIC ANALYSIS OF DARRIEUS VERTICAL AXIS WIND
TURBINE SYSTEMS FOR THE GENERATION OF UTILITY
GRID ELECTRICAL POWER
VOLUME II - THE ECONOMIC OPTIMIZATION MODEL

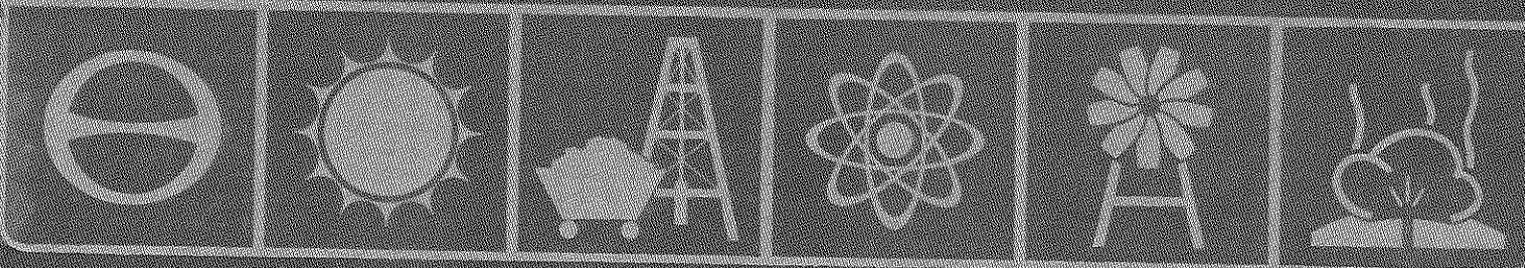
W. N. Sullivan

Prepared by Sandia Laboratories, Albuquerque, New Mexico 87185
and Livermore, California 94550 for the United States Department of
Energy under Contract AT(29-1)-789

Printed August 1979



Sandia Laboratories
energy report



Issued by Sandia Laboratories, operated for the United States
Department of Energy by Sandia Corporation.

NOTICE

This report was prepared as an account of work sponsored by the United States Government. Neither the United States nor the Department of Energy, nor any of their employees, nor any of their contractors, subcontractors, or their employees, makes any warranty, express or implied, or assumes any legal liability or responsibility for the accuracy, completeness or usefulness of any information, apparatus, product or process disclosed, or represents that its use would not infringe privately owned rights.

SAND78-0962
ECONOMIC ANALYSIS OF DARRIEUS VERTICAL AXIS WIND
TURBINE SYSTEMS FOR THE GENERATION OF
UTILITY GRID ELECTRICAL POWER
VOLUME II - THE ECONOMIC OPTIMIZATION MODEL

W. N. Sullivan
Advanced Energy Projects
Division 4715
Sandia Laboratories
Albuquerque, New Mexico 87185

Abstract

This report is part of a four-volume study of Darrieus vertical axis wind turbine (VAWT) economics. This volume describes a computer model of VAWT cost and performance factors useful for system design and optimization. The content and limitations of the model are outlined. Output data are presented to demonstrate selection of optima and to indicate sensitivity of energy cost to design parameter variations. Optimized specifications generated by this model for six point designs are summarized. These designs subsequently received a detailed economic analysis discussed in Volume IV.

An appendix is included with a FORTRAN IV listing of the model and a description of the input/output characteristics.

Acknowledgment

Specific aspects of this volume received the beneficial technical consultations of J. F. Banas, B. F. Blackwell, E. G. Kadlec, R. C. Reuter, and M. H. Worstell. More generally, the report represents a combination of effort from many contributions within and outside of Sandia Laboratories.

This study was monitored by D. D. Teague of DOE who provided substantial guidance with his many comments and criticisms throughout the study.

The support of all of these individuals is gratefully acknowledged.

Contents
Volume II - The Economic Optimization Model

	<u>Page</u>
Preface - Objective and Organization of the VAWT Economic Study	5
1. Introduction	7
2. Model Organization	11
3. Model Content	14
3.1 Performance Calculations	14
3.1.1 Aerodynamic Performance	14
3.1.2 Drive Train and Electrical Losses	18
3.1.3 Windspeed Distribution	20
3.1.4 Calculation of Annual Energy Production	20
3.2 Structural Constraints	22
3.2.1 Blade Structural Constraints	22
3.2.2 Tower Structural Constraints	27
3.2.3 Tiedown Structural Constraints	29
3.3 Component Cost and Weight Calculations	32
3.3.1 Rotor Blade Costs	32
3.3.2 Tiedown and Tower Costs	34
3.3.3 Transmission Costs	36
3.3.4 Generator and Electrical Controls	37
3.3.5 Installation Costs	39
4. Model Results	42
4.1 Cost per Kilowatt-Hour and Performance of Optimized Systems	42
4.1.1 Cost of Energy as a Function of System Size	43
4.1.2 Annual Performance and Total Cost of Optimized Systems	45
4.1.3 Meteorological Effects on System Cost of Energy	47
4.1.4 Sensitivity of Cost of Energy Results to Changes in Cost Formulation	47
4.2 Identification of Optimum Design Parameters	51
4.2.1 Rotor RPM	51
4.2.2 Rotor Solidity and Number of Blades	52
4.2.3 Rotor Height-to-Diameter Ratio	54
4.2.4 Rotor Ground Clearance	55
4.3 Specifications and Performance of the Point Designs	56
References	62
Glossary	64
APPENDIX - Version 16 of the Economic Optimization Model User Manual	70
A.1 Definition of Input Data	71
A.2 Definition of Output Data	73
A.3 Description of Subroutines	74
A.4 Complete FORTRAN IV Listing	75

Preface - Objective and Organization of the Vertical Axis
Wind Turbine (VAWT) Economic Study

The ultimate objective of the VAWT economic study is to determine as accurately as possible the profitable selling price of Darrieus vertical axis wind energy systems produced by a typical manufacturing and marketing firm. This price may then be compared to the electrical utility energy saved by the system to allow potential users to assess the usefulness of the VAWT concept. The basic approach for assessing the selling price is through a detailed economic analysis of six actual system designs. These designs cover a wide range of system size points, with rotor diameters from 18 to 150 ft., corresponding to approximate peak output ratings from 10 to 1600 kW. All these systems produce 60 Hz utility line power by means of induction or synchronous generators coupled mechanically to the rotor and electrically to the utility line.

Two independent consultants in parallel conducted the economic analyses of these point designs. A. T. Kearney, Inc., a management consulting firm, provided analyses for the four largest point designs; Alcoa Laboratories considered all six design points. Both studies attempt to determine a reasonable selling price for the various systems at several production rates ranging from 10 to 100 MW of peak power capacity installed annually. In addition, the consultants also estimated the costs of constructing one or four preproduction prototypes of each point design. Toward this objective, the consultants considered a hypothetical company to procure components; perform necessary manufacturing; and manage the sales, marketing, delivery, and field assembly of the units. Profits, overhead, and administrative costs for this hypothetical company are included in estimating the appropriate selling price for each point design.

Sandia Laboratories selected the basic configurations of the point designs (i.e., the number of blades, blade chord, rotor speed, etc.) and developed specifications for the configurations using an economic optimization model that reflects the state-of-the-art in Darrieus system design. The computer-adapted optimization model uses mathematical approximations for the costs of major system elements and the energy collection performance of the system. The model effects cost vs performance trade-offs to identify combinations of system parameters that are both technically feasible and economically optimal.

System configurations identified by the optimization model served as a starting point for all the point designs. Sandia Laboratories completed the designs for the four largest systems (120, 200, 500, and 1600 kW) and Alcoa Laboratories prepared the two smallest systems (10 and 30 kW). The level of detail associated with each design

is commensurate with an adequate determination of component costs and not necessarily with what is required for actual construction of the systems.

This final report is divided into four separate volumes, corresponding to overall organization of the study:

- Volume I The Executive Summary - presents overall conclusions and summarizes key results.
- Volume II Describes the economic optimization model including details of system performance calculations and cost formulas used in the optimization process. The model-estimated costs per kilowatt hour of the optimized systems are presented as a function of the rotor diameter, and the dominant cost and performance factors influencing the results are discussed. The volume concludes with a tabulation of optimized performance and physical characteristics of the point designs.
- Volume III Presents the actual point designs and discusses major design features. Tabular data on energy production, component weights, and component specifications are included.
- Volume IV Summarizes results provided by the cost consultants' analyses, interprets observed trends, and compares results with those from the economic optimization model.

1. Introduction

In any wind energy system, many variables such as the rotor diameter, blade chord, number of blades, rotor speed, and rated power must be specified to define that system. The process of designing particular Wind Energy Conversion Systems (WECS) must start from a specific selection of these system variables. The economic optimization model was developed as a design tool to aid in selecting optimal combinations of Darrieus vertical axis wind turbine (VAWT) system specifications. This report discusses the content of the model and applies it to determine specifications for six point designs which subsequently received a detailed economic analysis discussed in Volume IV.

The basic turbine configuration investigated is shown in Fig. 1.1 along with nomen-

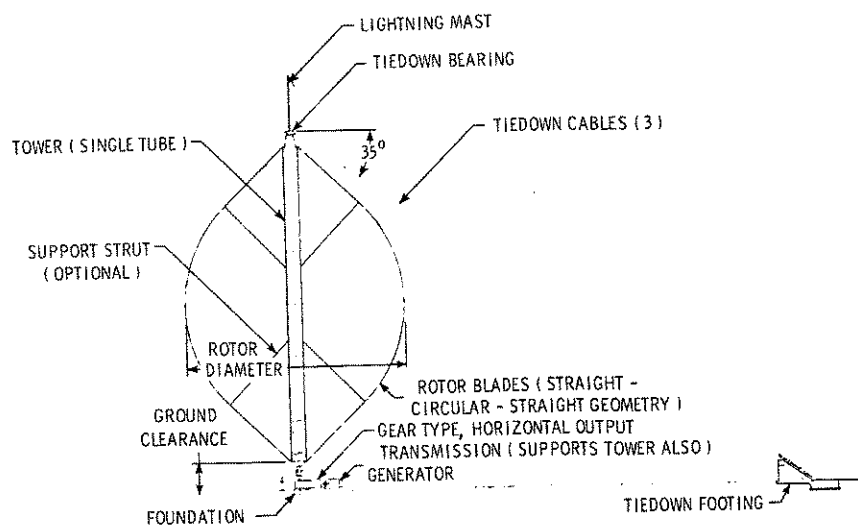


Figure 1.1 - Basic Turbine Configuration and Nomenclature

clature* used throughout this study. Primary features of the basic configuration are evident from this figure. This basic configuration is not substantially different from Darrieus systems designed and built in the past by Sandia Laboratories, the Canadian National Research Council, and others. The major differences are the elimination of the lower support base above the transmission (axial loads are taken out through

*A glossary at the end of this volume defines additional terms frequently used in this study.

the transmission), and the use of three (rather than four) tiedown cables. The configurational variables which have been investigated in this study are the blade chord, number of blades, the use of struts, height-to-diameter ratio, rotor rpm, ground clearance, and rotor diameter. The range of the variables was left open, with the appropriate limits determined by the trends observed in the cost of energy.

Several ground rules have been incorporated into the economic model, most significant of which are summarized in Table 1.1. These rules reflect an attempt to reduce cost and performance uncertainties that increase considerably with increased generality. Although there is no intention to conclude that concepts excluded by these ground rules may not offer economic or technical advantages, the ground rules do reflect the current state-of-the-art in Darrieus turbine design and serve as a reasonable starting point for this analysis.

The cost estimates in the optimization model are best interpreted as "1000th unit" costs as utilized in other^{1,2*} DOE-sponsored economic studies. There are no learning curves or other quantity discounts imbedded in the model cost formulas. This exclusion avoids the substantial uncertainties involved in generalizing a cost formula to include production quantity effects which are valid over a wide range of component sizes and specifications. If production quantity effects need to be assessed, component-by-component analysis of a particular design is the recommended course of action.

An important feature of this model is the inclusion of structural constraints on the major rotor elements -- specifically the blades, tower, and tiedowns -- because these elements should be sized according to structural rather than economic limits. For example, a tiedown cable will obviously be less expensive as its diameter and breaking strength decrease, but there are certain structural limitations that should govern cable size. The same applies for tower and blade elements. Structural constraints are incorporated in the model to prevent convergence to economically attractive solutions that are not structurally sound.

Application of this model to select point design configurations showed that, whereas some variables had a marked effect on costs per unit of energy produced, others did not. In the case of variables found in the model to be very weakly effective on cost, the following basic preferences governed the final selection: 1) physical simplicity over the more complex, 2) design similar to past experience over untried design, 3) lower weight, and 4) higher energy collection per unit of swept area. Application of one or more of these rules was sufficient for a final selection of variables for the point designs.

*Superscripts denote references at the end of this report.

Table 1.1
Optimization Model Major Ground Rules

- Rotor to operate at constant rpm, controlled by the utility grid through a synchronous or induction generator.
- Blade construction from constant cross section, NACA 0015, thin-walled, hollow aluminum extrusions, using manufacturing techniques existing in the United States.
- Single rotating tower of tubular cross section, supported at the top by a three cable tiedown system.
- All structural components to be stressed below 6000 psi vibratory stress in 60 mph rotor centerline windspeeds at normal operating rotor rpm.
- Parked rotor survival windspeed of 150 mph at the rotor centerline.
- Cost estimates based on recurring component costs expected for an established production industry.
- Total annual system cost, including operation, maintenance, and financing assumed to be 15% of total capital cost.*
- Optimization based on minimizing annual system cost per unit of energy supplied.
- 15 mph average windspeed distribution used for point design optimizations.
- Wind shear exponent of 0.17 from a reference height of 30 feet used for energy calculations.

*The Executive Summary (Volume I) of this study uses a different formula for calculating the cost of energy to facilitate comparison of results with other DOE-sponsored economic studies.

Probably the most significant result of this study concerns the effect of system size on the cost of energy. The cost of energy was found to be surprisingly insensitive to system size for rotor diameters from 50 to 150 ft., (corresponding to approximately 100 to 1500 kW ratings, respectively), with a definite trend towards less cost-effectiveness on either side of this range. The results also indicate an economic preference for rotors with two blades, no struts, and height-to-diameter ratios between 1.25 and 1.5. These features have been incorporated in the point designs discussed in Volume III of the overall study.

Many computational and conceptual simplifications are necessary to develop this model and to yield a compact, understandable instrument. This is the main disadvantage to the computer modeling approach of economic analysis. It is important for the user to be familiar with the strengths and weaknesses of the model and to use judgment in interpreting results.

There is also the problem of continuing maintenance of the model as correctable weaknesses are discovered or as new cost and performance data are available. There have been 16 different versions* of the economic optimization model developed during the course of this study. Each version represents an update to the cost or performance calculations motivated by the appearance of new information. The future usefulness of this model depends on the user's willingness to continue updating and improving the model as more reliable data on wind turbine economics appear.

In what follows, Section 2 describes the basic organization of the program. Section 3 gives details on the program components; and Section 4 presents results, including the definition of point designs. A complete FORTRAN IV listing of the optimization model is attached as an appendix.

*The June 1978 version, referred to as "Version 16", described in this report, is the latest available at the time of writing.

2. Model Organization

The optimization model has been implemented on a time-sharing computer system. This permits interactive use of the program through a keyboard.

The model is not strictly an optimization program in that "best" combinations of variables are not selected entirely by the computer. Rather, a set of dependent variables such as component costs and weights, and annual energy output are calculated and displayed based on the user's choice of independent variables. The user actually selects the optimum configuration by trying various combinations of independent variables. This approach, which retains a judgmental factor in applying the model, avoids convergence to mathematical optima that are impractical or artificial because of subtle inaccuracies in the basic economic modeling.

Program organization is shown in Fig. 2.1. Input variables on the left are selec-

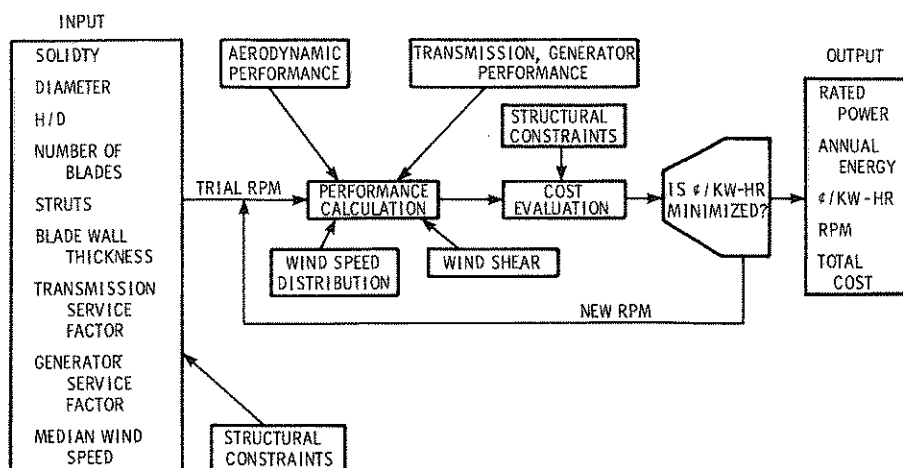


Figure 2.1 - Economic Optimization Model Organization
(See Glossary for Definition of Terms)

ted by the user. From these choices, the aerodynamic and electrical performance is calculated, followed by estimates of component costs. The turbine rpm is usually varied to minimize the system cost per unit of energy produced, although an option is available to permit selection of the rpm as an input variable. This option was found to be important for assessing performance of a system constrained to a particular rpm by transmission or structural limitations.

The choice of independent variables for input to the program is not unique. For example, rated power^{1,2} could have been used as the fundamental parameter governing the size of the system. However, experience indicated that using the physical rotor dimensions (diameter, blade chord, number of blades, etc.) is more convenient. The reason is that when rated power is used as input, very slight changes in performance or cost calculations yield completely different optimized rotor dimensions. Alternatively, with rotor dimensions fixed on input, program alterations affect primarily the rated power, annual energy, and optimum rotor rpm. These latter changes are much easier to incorporate into an ongoing design than are changes in the rotor dimensions.

Structural constraints are introduced into the program in two different ways. The blades are constrained on input by considering only structurally adequate possibilities to begin with. The tower and tiedowns are actually dimensioned within the main program, with dimensions selected to meet minimum structural requirements.

A typical input sequence is shown in Fig. 2.2. The user responds to questions with appropriate input data. Typical output is shown in Fig. 2.3. Computation time is negligible and the user may conduct many iterations, the primary limitation being the speed of the output terminal. For rapid evaluation of many combinations of input variables, a brief output option is available that prints only the last three lines of the usual output.

A user's manual for this program is included in an appendix at the end of this volume. The manual defines the input and output data in some detail. A complete FORTRAN IV listing of the program is also in the appendix.

```

ENTER DIAMETER,NUMBER OF BLADES,H/D,STRUTS
? 55.,2.,1.5,0.
ENTER TURBINE SOLIDITY,BLADE WALL THICKNESS RATIO
? .134,.01
ENTER GEN.,TRANS. SERVICE FACTORS,LINE VOLTAGE
? 1.,1.,460.
BRIEF OUTPUT?
? N
WANT OPTIMIZED RPM?
? Y
ENT: MED. W/S,AIR DENS.,XPON,HCLR
? 15.,.076,.17,7.

```

Figure 2.2 - Input Sequence for the Economic Optimization Model

```

VERS16,6/30/78, 55.X 83. FT ROTOR 460.VOLTS
CPK,CPMAX,RE-- .00785 .38598 .18069584E+07
KMR TIP SPEED RATIOS-- 3.01 5.76 11.47
PEAK OUTPUTS(KW):ROTOR,TRANS,GEN-- 124.19 119.22 109.70
PEAK TORQUE,LO SPEED SHAFT-- 16971.9
RATED WIND SPEED(MPH@ 30'REF)-- 30.96
TOTAL ENERGY-- 237999. 15.MPH MED. WIND SPEED

CHORD,TURBINE SOLIDITY-- 23.673 .134
BLADE WALL THICKNESS RATIO,WALL THICKNESS-- .010 .237
UNSTRUTTED TURBINE,H/D =1.50
BLADE GROUND CLEARANCE-- 7.00
MAX. TORQUE CAPACITY,TRANS-- 16972.
MAX ELECTRICAL CAPACITY,GEN-- 110.
TOWER DIA,WALL THICKNESS-- 3.5 .074
DIAMETER,RPM,TIPSPEED-- 55.00 51.52 148.36
NET AXIAL LOAD INTO BASE-- 43576.45

ITEM COST($ ) PERCENT OF TOTAL WEIGHT $/LB
BLADES 9124.41 17.5 3439. 2.65
TOWER 7232.40 13.9 4822. 1.50
TIEDOWNS 3916.43 7.5 1567. 2.50
TRANS 7893.99 15.2 2037. 3.88
GENERATOR 8993.41 17.3 1359. 6.62
FOUNDATION 2211.99 4.2
ASSEMBLY 12684.49 24.4
TOTAL 52057.12 100.0 13222. 3.94
NORMALIZED($/KW-HR)-- 3.28
CHANGES OR <CR> TO GO
?

```

Figure 2.3 - Output of the Economic Optimization Model (Version 16). Input and Output Terminology Are Defined in the Appendix of This Volume

3. Model Content

3.1 Performance Calculations

The performance calculations in the model consist of several parts. These are: (1) calculation of aerodynamic performance of the rotor, (2) calculation of drive train and electrical losses, (3) input of the windspeed distribution with correction for wind shear, and (4) integration of performance characteristics over the windspeed distribution to obtain annual energy production. Each aspect of the performance calculation will be considered separately.

3.1.1 Aerodynamic Performance -- The problem of aerodynamic performance is determining appropriate performance curves for a variety of rotor parameters, such as the height-to-diameter ratio, the solidity,* the blade Reynolds number, and the ratio of tip to windspeed. Experience with wind tunnel tests³ and aerodynamic analyses have indicated that all these parameters can significantly affect rotor performance characteristics.

The classical performance measure for wind turbines is the power coefficient (C_p) defined as the ratio of turbine shaft power per unit of projected turbine area to the power in the undisturbed wind per unit area. In mathematical terms,

$$C_p = \frac{P_t/A}{\frac{1}{2}\rho V_\infty^3} ,$$

where P_t is the rotor shaft power, A is the projected area, ρ is the air density, and V_∞ is the ambient windspeed. The power coefficient depends most strongly on the tip speed ratio, λ , and is usually expressed as a function of λ , with the other rotor variables such as blade Reynolds number, height-to-diameter ratio (H/D), and solidity held constant.

In the optimization model, the power coefficient curve needs to be simplified so that it may be appropriately varied as a continuous function of the rotor variables. This has been effected by using a five-parameter curve, shown in Fig. 3.1. The five

*Throughout this report, the solidity is defined as the ratio of total blade area to the projected area of the rotor. The blade area is $n \cdot BL \cdot C$, where n is the number of blades, BL is the blade length, and C is the blade chord. The projected turbine area is approximated by $A = \frac{8}{3} R^2 H/D$, with R being the turbine radius, and H/D being the height-to-diameter ratio.

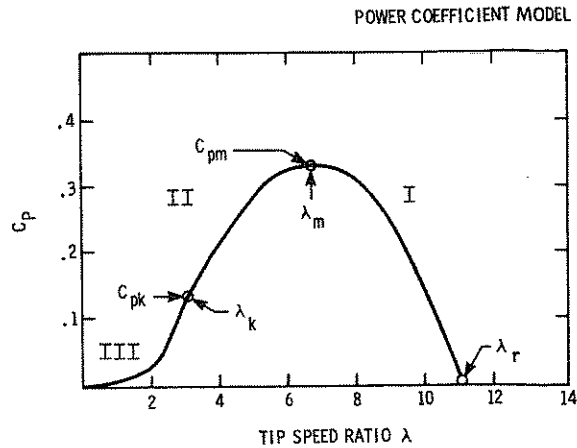


Figure 3.1 - Parameterization of the Power Coefficient Curve

parameters are: the "runaway" tip speed ratio, λ_r ; the maximum power coefficient, C_{pm} ; the tip speed ratio, λ_m , corresponding to C_{pm} ; the value of power coefficient, C_{pk} , at which the ratio C_p/λ^3 is a maximum; and λ_k , the value of the tip speed ratio corresponding to C_{pk} . The significance of these first three parameters is reasonably self-evident, but the latter two are unusual. The C_{pk} and λ_k govern the peak power and rated windspeed, respectively, which occur when the rotor is operated at constant rpm⁴ as in the utility grid application. Defining the quantity $K_p = C_{pk}/\lambda_k^3$, it follows from the definitions of C_{pk} and λ_k that the peak aerodynamic power in a constant rpm application is

$$P_{max} = K_p \left[\frac{1}{2} \rho A (Rw)^3 \right]$$

and occurs at a rotor centerline windspeed

$$V_{rated} = Rw/\lambda_k \quad ,$$

where Rw is the fixed tip speed of the rotor.

The actual C_p curve shown in Fig. 3.1 is a smooth function going through the five parameters discussed. In Region I, a parabola is used, going through C_{pm} and 0 at λ_m and λ_r , respectively, with zero slope at C_{pm} . In Region II, a similar parabola is used through the points at C_{pm} and C_{pk} . Region III uses a curve, $C_p = B\lambda^n$, where B is selected so that $C_p = C_{pk}$ at $\lambda = \lambda_k$, and n is taken to be 3.5. The value of n governs the performance of the rotor above rated windspeed.

In constructing this C_p curve model, the ultimate objective is to create a power vs windspeed curve for any fixed value of $R\omega$ that is representative of Darrieus aerodynamic performance. This is because the power vs windspeed characteristic is what is actually used to determine annual performance. Figure 3.2 shows the power vs windspeed

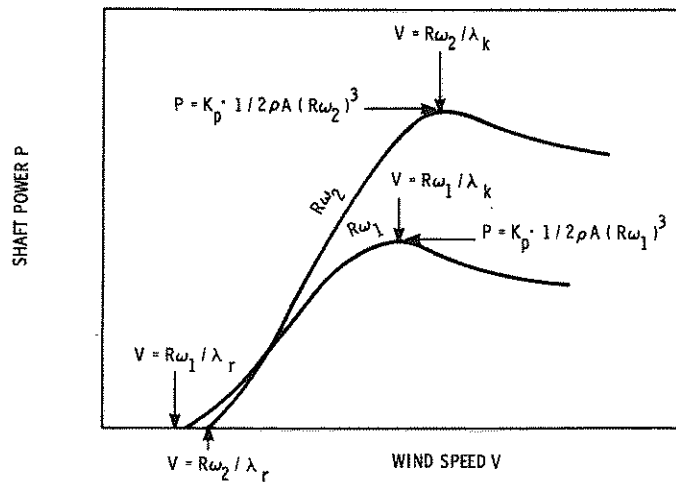


Figure 3.2 - Power vs Windspeed Characteristic for the Model Power Coefficient of Fig. 3.1

characteristic following from a model C_p curve for two tip speeds, $R\omega_1$ and $R\omega_2$. The influence of the five parameters used to specify the C_p curves is indicated on this figure. Note that as discussed in other reports,⁴ the output power is limited to a maximum value that is quite dependent on the particular constant rotor speed selected for the system. The shape of this curve is very similar to that measured from field and wind tunnel tests on the DOE/Sandia 17 meter, 5 meter, and 2 meter Darrieus turbines as well as the Canadian Magdalen Island machine.^{5,6,7} The value of n in Region III of the C_p curve governs the performance of the rotor above rating. If n were exactly equal to 3, the power output would be constant above rating. The choice, $n = 3.5$, was made to produce a fall-off in power above rating roughly similar to that observed experimentally.

The remaining part of performance modeling involves determining the value of the five power coefficient parameters as functions of the turbine solidity, H/D ratio, and the Reynolds number.* The multiple streamtube model,⁸ with a modification to account for variations in the local blade Reynolds number, was applied⁹ to determine the power

*The Reynolds number, called Re_c , is defined as $Re_c = (R\omega)C/\nu$, where C is the blade chord and ν is the kinematic viscosity of air.

coefficient parameters. In applying the streamtube model, comparison with experimental data on 2 meter wind turbines indicated reasonable agreement except for a tendency to overpredict the runaway tip speed ratio, λ_r . The values of λ_r were reduced from 10 to 30% in the optimization model to fit the 2 meter experimental data.

An interpolation routine was developed for intermediate values of the power coefficient parameters from a multiple streamtube determination of the parameters at discrete solidities (0.05, 0.13, and 0.25), H/D ratios (1.0, 1.25, and 1.5), and a range of Reynolds numbers. This interpolation routine, CPPARM, is used in the optimization model for solidities from 0.05 to 0.25, H/D ratios from 1.0 to 1.5, and Reynolds numbers from 1×10^5 to 3×10^6 . NACA 0015 airfoil data are used in the versions of CPPARM in this study, although versions are available for the NACA 0012.

Typical results from the application of CPPARM (Fig. 3.3) indicate the effect of

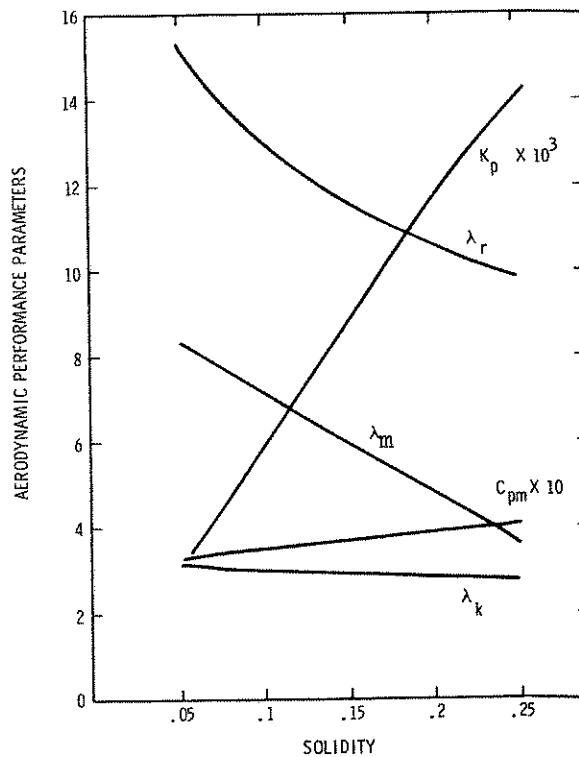


Figure 3.3 - Solidity Effects on Aerodynamic Performance:
From Multiple Streamtube Model, $Re_c = 3 \times 10^6$,
NACA 0015

turbine solidity on the five performance parameters. Note the tendency of λ_k , λ_m , and λ_r tip speed ratios to increase with decreasing solidity, as is typical for all wind turbines. This effect tends to increase rotor speed, an advantage in that the required transmission capacity tends to be reduced. This beneficial effect is offset by the reduction in C_{pm} and K_p , which reduces the total energy collected by the rotor.

Aerodynamic performance calculations are an important part of the optimization model. The total annual energy collected and the optimum rotor rpm are directly related to the five parameters generated by CPPARM. There is, therefore, a need to experimentally verify and update the results predicted by CPPARM as a part of any maintenance program for the optimization model.

3.1.2 Drive Train and Electrical Losses -- Losses in converting aerodynamic torque to electrical energy occur in the mechanical speed increaser and the generator.

In the speed increaser, a fixed-loss model is used that assumes a fixed-power loss for all loading conditions in the transmission. The magnitude of power loss is taken to be a percentage of the low speed shaft rated power of the transmission. The optimization model assumes the fixed loss is 2% of rated transmission power per stage of gears. The number of transmission stages required is determined using a maximum gear ratio of 6:1 per stage. The high speed shaft is assumed to turn at 1800 rpm and the low speed shaft at rotor rpm for calculating the number of stages required.

At fractions of rated transmission loads, where the system operates most of the time, the efficiency of the transmission falls off rapidly (Fig. 3.4) as a fixed loss is

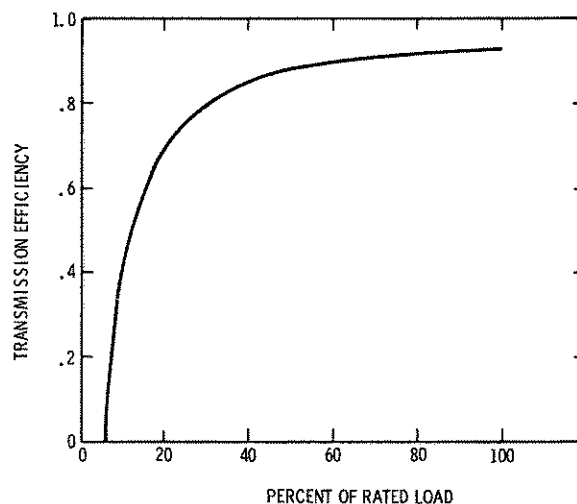


Figure 3.4 - Mechanical Transmission Efficiency, Fixed Loss Model

always subtracted from aerodynamic power input to the speed increaser. This differs considerably from the fixed efficiency models used in other wind turbine system studies.^{1,2} The application of the fixed loss model is based on the fact that transmission losses are primarily due to viscous friction,¹⁰ and in the constant rpm application, these losses are only weakly dependent on transmitted torque.

A capability exists to assign service factors to the transmission. This service factor is the ratio of the continuous input power capacity of the transmission to the peak power output of the rotor. Service factors other than unity are sometimes necessary to fit a cataloged transmission to a particular WECS or to provide additional capacity for unusual torque inputs from the rotor, such as torque ripple.^{11,12} This service factor influences the loss model by changing the power capacity and hence the fixed loss of the transmission.

The rated load efficiency of the generator depends on the rated power of the generator. The electrical loss at rated load² is taken to be

$$R_{\text{loss}} = 0.05(1000/P_{\text{rated}})^{0.215}$$

where P_{rated} is the rated generator power in kilowatts. This formula is compared in Fig. 3.5 with the Smeaton Handbook recommendation. The simple formula agrees rea-

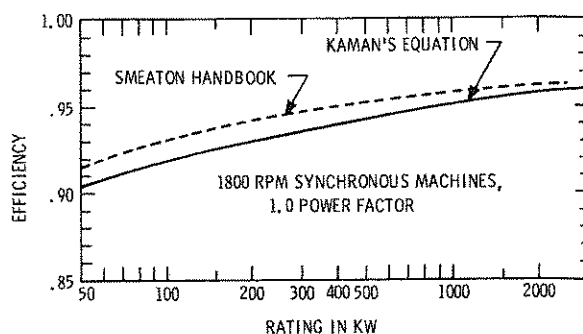


Figure 3.5 - Efficiency of Synchronous Generators at Rated Conditions

sonably well with these data.

At fractions of rated load, the absolute loss is assumed² to decrease parabolically to half the loss at rated load as the load decreases to zero; i.e.,

$$\text{Loss} = [0.5(P_0/P_{\text{rated}})^2 + 0.5] R_{\text{loss}}$$

where PO is the electrical output power. Note that the efficiency of the generator, $PO/(Loss + PO)$, is reduced considerably for operation at fractions of full load.

Service factors may be assigned to the electrical generator for the same reasons they are used on the transmission. Generator service factors above unity tend to increase the electrical losses by increasing the time the generator is fractionally loaded.

While this loss model is for synchronous generators, the same model is assumed to apply for induction generators.

3.1.3 Windspeed Distribution -- Three wind duration curves are imbedded in the model. These correspond, respectively, to 12, 15, and 18 mph annual median windspeeds measured at a 30 ft. reference height. These duration curves, shown in Fig. 3.6, are identical to those used in earlier DOE-sponsored systems studies on horizontal axis WECS.^{1,2}

A wind shear correction is applied to these data to adjust the distribution velocity, V_{ref} , to a rotor centerline velocity, V_{cl} . The centerline velocity is then used in calculating aerodynamic output of the rotor. The standard correction

$$V_{cl} = V_{ref} (H_{cl}/H_{ref})^{XPON}$$

is used, where H_{cl} is the height of the rotor centerline, and H_{ref} is the reference height for the speed distribution. The value of XPON is 0.17 unless otherwise noted. A user option exists to change the exponent if desired.

While all results presented in this report are for the 12, 15, or 18 mph distributions of Fig. 3.6, performance characteristics may also be determined for a Rayleigh distribution at user discretion. The Rayleigh distribution has the advantage that any desired mean windspeed may be input.

3.1.4 Calculation of Annual Energy Production -- Annual energy output is always calculated at a fixed rotor tip speed, Rw , corresponding to the synchronous operating speed of the turbine. For a given value of tip speed, the Reynolds number is calculated and CPPARM produces the five aerodynamic performance parameters.

The value of K_p (see Section 3.1.1) governs the peak aerodynamic output of the rotor,

$$P_{tmax} = \left[\frac{1}{2} \rho A (Rw)^3 \right] K_p$$

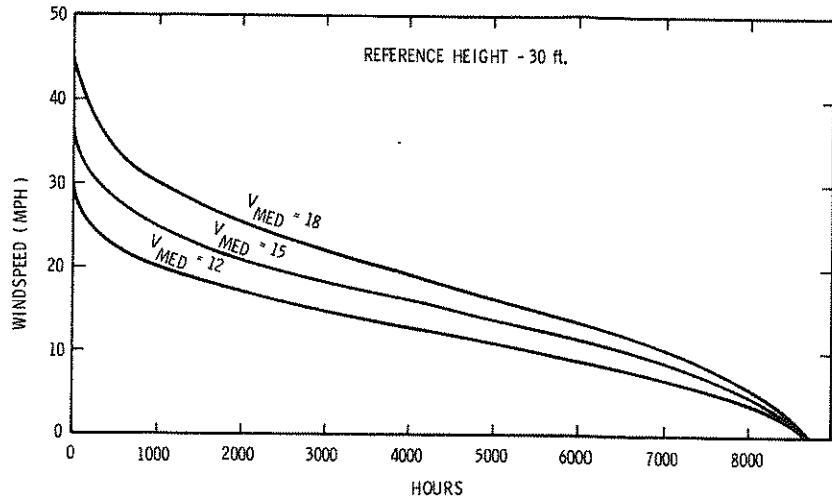


Figure 3.6 - Annual Windspeed Duration Curves Used in Economic Optimization Model. The Curve Represents the Number of Hours in a Year That the Windspeed Exceeds a Specified Value

The projected area of the rotor, A , is given for different radius and H/D ratio rotors by $A = 8/3 R^2 (H/D)$. This formula follows from a parabolic approximation to the blade geometry.¹³ The air density, ρ , is generally taken to be 0.076 lbm/ft^3 , which corresponds to a standard day at sea level.

Peak aerodynamic output is used to determine transmission and generator power ratings. System power output as a function of the centerline windspeed is

$$P_s(V_{cl}) = P_t(V_{cl}) - \text{transmission loss} - \text{generator loss},$$

with

$$P_t(V_{cl}) = \frac{1}{2} \rho A V_{cl}^3 C_p(\lambda); \lambda = R\omega/V_{cl} \quad .$$

Transmission and generator losses are calculated as discussed in Section 3.1.2.

Annual energy is determined by integrating the system power over the centerline windspeed duration curve, $V_{cl}(t)$,

$$E_s = \int_{t_{\min}}^{t_{\max}} P_s(V_{cl}) dt \quad .$$

In this formula, the time, t_{max} , corresponds to the cut-in velocity on the duration curve; i.e., the lowest velocity for which $P_s(V_{cl})$ is positive. The time, t_{min} , corresponds to the cut-out velocity. Throughout this study, it is assumed that $t_{min} = 0$, as the maximum windspeeds on the duration curves are generally well below the 60 mph design windspeed of the rotor.

3.2 Structural Constraints

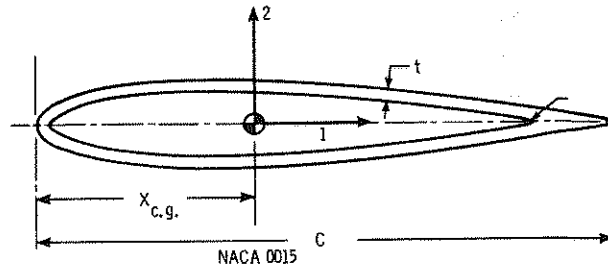
The major structural components of the vertical axis WECS (the blades, tower and tiedown cables) are constrained dimensionally in the optimization model to ensure compliance with minimum structural performance standards.

Several simplifying assumptions were made in establishing these constraints, as it is not possible to complete a complex structural analysis of each component within the optimization model. Thus, while the constraints do screen out designs that clearly are structurally inadequate, they are not intended to eliminate subsequent detailed structural analyses on each point design.

Structural constraints have a substantial impact on the overall optimization study because the basic dimensions (and hence the costs) of the rotor components are governed by the structural constraints. It is therefore recommended that this area receive attention in future research programs, with attention directed toward the refinement and confirmation of existing calculations.

3.2.1 Blade Structural Constraints -- The structural adequacy of a blade is a function of its chord, the mechanical inertias and area of the cross section, the rotor diameter and H/D ratio, and the physical properties (yield strength, elastic modulus, etc.) of the blade material. To limit the large number of possible variations among these blade characteristics, this study is restricted to aluminum extrusions of 6063-T6 material. A simplified cross section is used to calculate section properties. This section is simply a NACA 0015 hollow airfoil with uniform wall thickness (Fig. 3.7). Of course, extruded blades designed for this application typically have vertical webs to stabilize the forming of curved blade sections, but these vertical webs have only a small influence on cross section inertias. The advantage to this simple section is that mechanical cross section properties may be very easily calculated from the blade chord, C , and the wall thickness-to-chord ratio, $r = t/C$. Table 3.1 summarizes the simple calculations required to determine all the section properties for the blade of Fig. 3.6.

A set of minimum acceptable performance criteria is required to establish structural adequacy of the blade. The following criteria have been used in the optimization model:



- C = BLADE CHORD
- t = BLADE WALL THICKNESS
- $X_{c.g.}$ = DISTANCE FROM NOSE TO CENTER OF GRAVITY (CENTROID)
- I_E = EDGEWISE SECTION INERTIA = I_{22}
- I_F = FLATWISE SECTION INERTIA = I_{11}
- J = TWISTING STIFFNESS FORM FACTOR

Figure 3.7 - Blade Model for Determining Structural Constraints

Table 3.1
Property Values for Simplified Blade Section in Fig. 3.6

Quantity	Value
Flatwise Inertia I_F	$C^4 r 6.2 \times 10^{-3}$
Edgewise Inertia I_E	$C^4 r 1.7 \times 10^{-1}$
Twisting Stiffness to Edgewise Stiffness Ratio GJ/EI_E	0.036
Blade Centroid Location $X_{c.g.}$	0.49 C
Structural Area A_s	2.08 $C^2 r$
Enclosed Area	0.102 C^2

Notes: Units of structural quantities determined by the units of blade chord, C; r is the ratio of wall thickness to blade chord.

Property calculations use thin-wall approximations and should not be used for $r > 0.015$.

1. Vibratory trailing edge blade stresses due to edgewise blade loading less than the endurance limit at a "normal" operating condition of 150 fps tip speed with 60 mph winds.
2. Twisting deformations in the blade due to edgewise loading less than 2 degrees at the normal operating condition.
3. No blade collapse with a parked rotor with 150 mph centerline windspeeds normal to the blade chord.
4. Gravitational stresses less than 40% of yield (assumed to be 30,000 psi) in the parked, wind-off condition.
5. Flatwise stresses due to centrifugal and aerodynamic loads below the endurance limit at the normal operating condition.

The endurance limit for the vibratory blade stresses is taken to be 6000 psi (zero to peak) for the 6063-T6 extrusions. This is a very conservative estimate¹⁴ for a 10^7 cycle lifetime. Considering the infrequent nature of 60 mph winds, and the fact that vibratory stresses decrease to zero as windspeed is reduced¹⁵, the 10^7 cycle fatigue lifetime corresponds to considerably more actual rotor cycles.

There are, of course, many other structural criteria involved in designing a Darrieus rotor blade, but a blade design that meets these fairly severe criteria will, in all likelihood, be structurally acceptable. Notable in their absence as structural criteria are blade resonant frequency requirements; this is because the above conditions lead to blades that necessarily are quite stiff in both the flatwise and edgewise directions. This produces relatively high blade resonant frequencies, the order of two to three times the rotational frequency of the rotor. While these frequencies are not high enough to preclude significant aerodynamic excitation of blade resonances, the probability of such excitation is low. Also, the frequency spacing between the lowest blade modes is large enough to avoid any excitations that may occur by making small adjustments to the synchronous rotor rpm.

Given the structural performance requirements on the blade, it remains to estimate stress levels as a function of blade structural properties. This has been done by extending results from finite element analyses¹⁶ of the 17 meter research turbine. Dimensional analysis is used to deduce performance of geometrically similar rotors with different blade properties. An example of this approach is shown in Fig. 3.8. Results for the edgewise bending stress^{*} at the blade root are expressed in dimensionless form. The dimensionless stress is

*Edgewise bending stresses are estimated with quasi-static loading; i.e., dynamic effects are neglected. This procedure is justified if blade and system resonant frequencies are well above the aerodynamic excitation frequencies. If this is not the case, the result should be interpreted cautiously.

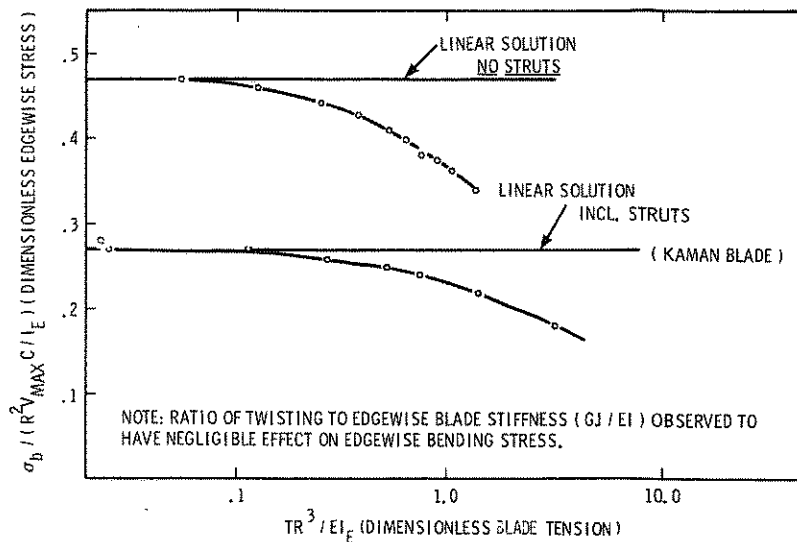


Figure 3.8 - Edgewise Bending Stress as a Function of Blade Tensile Load, T

$$\sigma_b / (R^2 V_{\max}^2 C / I_e) ,$$

where σ_b is the dimensional stress, R is the turbine radius, V_{\max} is the edgewise aerodynamic loading per foot of blade at the rotor centerline, L is the distance from the centroid of the blade to the trailing edge, and I_e is the cross section edgewise moment of inertia. Two cases are shown for rotors with or without 17 meter-type support struts. A centrifugal stiffening effect is shown in Fig. 3.8. The amount of centrifugal stiffening depends on the rotationally induced blade tension, T , expressed in dimensionless form. The maximum aerodynamic load, V_{\max} , is estimated with the single streamtube model.^{8,17} The load, V_{\max} , and hence the edgewise bending stress, depend on the wind and tip speed associated with the operating condition and the turbine geometry. For a fixed set of operation conditions, the load, V_{\max} , is almost directly proportional to the blade chord, C .

Similar dimensionless curves have been developed for other aspects of structural performance, including parked blade gust loading, gravitational stresses and deflections, blade twist due to edgewise loading, and flatwise blade stresses. These curves are used like the edgewise stress curves to estimate performance of many turbine types.

Blade stress levels and deflections become progressively higher for a fixed ratio of blade wall thickness-to-chord length as the chord-to-radius ratio (C/R) is reduced. This is because blade cross section properties deteriorate rapidly with reduced chord (see Table 3.1). Thus, there is some minimum value of C/R at which the structural performance is just adequate. Because of the dependence of the blade section properties on the blade wall thickness-to-chord ratio, $r = t/C$, this minimum possible C/R depends on r .

A curve of minimum possible C/R's as a function of r (Fig. 3.9) is shown for

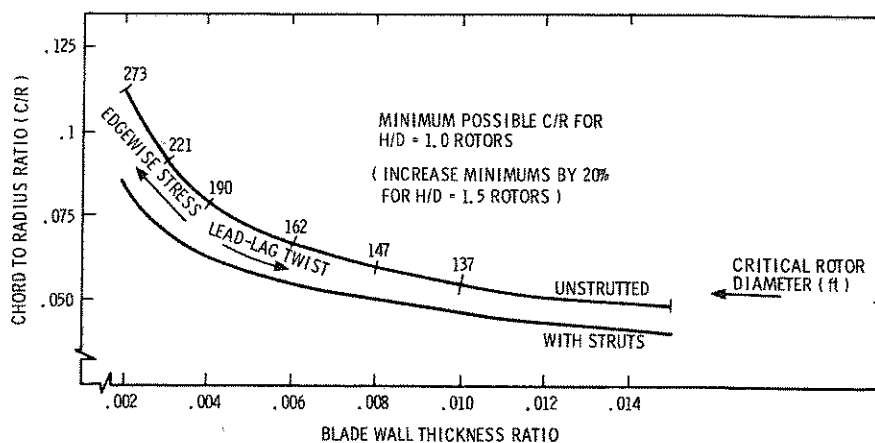


Figure 3.9 - Chord-to-Rotor Radius Ratio Minimums as a Function of Blade Wall Thickness

rotors with a H/D ratio of 1.0. The structural criterion that is first violated at the minimum C/R is indicated on the figure. Note that for large wall thickness-to-chord ratios, the blade twist condition is dominant, while thinner walled blades are vulnerable to edgewise stresses. Also indicated on the figure is a "critical rotor diameter," the rotor diameter above which gravitational stress condition is violated. The critical diameter may be increased by increasing the blade C/R.

Modifying the definition of minimum acceptable performance will naturally change the minimum possible C/R. Examination of performance criteria indicates that the first four criteria are dominant and of nearly equal importance. Thus, a significant change in minimum possible C/R would require reduction in the performance standards on all of the first four conditions.

It should be emphasized that the results shown in Fig. 3.9 are only valid approximations for the aluminum extruded blade section of Fig. 3.6. Using other materials or a different section geometry may change the minimum possible C/R.

Support struts as used on the DOE/Sandia and the Canadian National Research Council (NRC) Magdalen Island turbines tend to decrease the minimum possible C/R because the struts contribute to improved edgewise stiffness, parked buckling resistance, and reduced gravitational stresses. This effect is indicated on Fig. 3.9, based on analyses of the strutted 17 meter turbine. The critical diameters for gravitational loads are not shown on this figure because they are generally above 500 ft. and out of the range of interest in this study.

For a blade of given chord and wall thickness, rotors with larger H/D ratios are expected to be weaker in all directions due to the increased aspect ratio (blade length-to-chord ratio) of the blades. In analyzing H/D > 1 rotors in the optimization model, the minimum permissible C/R has been increased 20% to account for this effect. This increase is a judgmental estimate that is currently being examined with new finite element models for H/D = 1.5 rotors.

3.2.2 Tower Structural Constraints -- The tower is defined as the rotating support structure between the upper tiedown bearing and the base support above the transmission. It is a single tube designed to transmit aerodynamic torque from the blades and axial tiedown reactions into the transmission. Tower construction is assumed to be of mild steel with a cylindrical cross section and uniform wall thickness.

The following structural criteria, based on the formulas in Table 3.2, are used to evaluate towers:

1. General and local buckling loads are at least 10 times greater than tower axial loads.
2. Torsional and bending tower natural frequencies are above 4/rev at a rotor tip speed of 200 fps.
3. Tower axial stresses are below 6,000 psi.

Generally, these conditions are in decreasing order of dominance. The buckling condition safety factors are high to account for eccentricities and local flaws in the structure that inevitably occur in any real design.

The basic structural parameters involved in tubular tower selection are the tower diameter and its wall thickness. Many possible combinations of these parameters can satisfy the structural criteria; however, it was observed that a unique combination resulted if the requirement of minimum tower volume (weight) was added. Such minimum volume towers are used in the optimization model.

Although the tower dimensions resulting from application of this model do meet structural requirements, they may violate other practical considerations. For example, a tower diameter should not be a substantial fraction of the rotor diameter, or flow blockage may occur. Excessively thin or thick walls may be difficult or impossible

Table 3.2
Formulas Used for Determining Tower Performance

Critical general buckling load, P_{crg} :

$$P_{crg} = \left(\frac{\pi^3 E}{64 L^2} \right) D_o^4 [1 - (D_i/D_o)^4]$$

Critical local buckling load, P_{crl} :

$$P_{crl} = \left(\frac{\pi E}{4 \sqrt{3(1 - \nu^2)}} \right) D_o^2 (1 - D_i/D_o) [1 - (D_i/D_o)^2]$$

First tower bending frequency, f_b :

$$f_b = .39 \sqrt{E/\rho L^4} D_o [1 + (D_i/D_o)^2]^{\frac{1}{2}}$$

First tower torsional frequency, f_t :

$$f_t = (G/\pi L J_b)^{\frac{1}{2}} D_o^2 [1 - (D_i/D_o)^4]^{\frac{1}{2}}$$

Static compressive stress, σ_c :

$$\sigma_c = \text{net axial load} / (\pi/4) D_o^2 [1 - (D_i/D_o)^2]$$

where

D_o = tower O.D.

D_i = tower I.D.

L = tower length

E = Young's modulus

G = shear modulus

ν = Poisson's ratio

J_b = polar mass moment of inertia of tower and blades

to manufacture. These special problems require some user care in interpretation of results to avoid conflicts.

The mechanics of calculating tower dimensions are automatically carried out in the optimization model. Axial tower load sources accounted for include the tiedown reactions, the axial component of centrifugal blade loads, and the weight of the tie-downs, tower, and blades. The tower length is calculated from the rotor geometry, including any additional ground clearance specified by the user. The formulas in Table 3.2 are used to calculate critical buckling loads, resonant frequencies, and stresses.

Typical results for minimum volume, structurally adequate tower dimensions are shown in Fig. 3.10. It is noteworthy that the tower proportions suggested by this

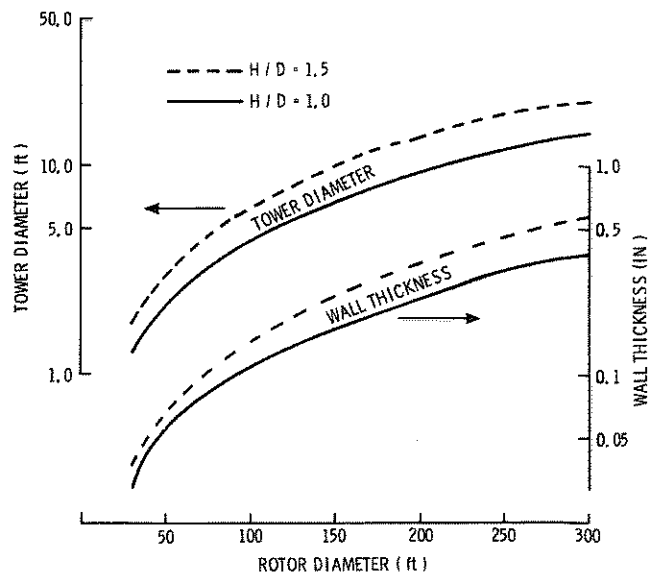


Figure 3.10 - Dimensions of Minimum Volume Towers Satisfying the Structural Criteria Discussed in Section 3.2.2

model have larger diameters and much thinner walls than were used on the Sandia 5 meter and 17 meter prototypes. These large diameter, thin-walled towers are substantially lighter than the smaller diameter, thick-walled tubes used in the past.

3.2.3 Tiedown Structural Constraints -- The cable tiedown system provides a simple, inexpensive way to support the rotor against overturning loads. Two properties

of the cable are subject to structural constraints -- the cable diameter and the pretension. The cable diameter has direct impact on cable cost; the pretension influences tower and foundation costs.

The structural constraints imposed in the optimization model are derived from a scaling analysis of the 17 meter research turbine cable system.^{18,19} A major exception to this rule is the use of three cables in this study rather than the four used on the 17 meter system. This change was made to simplify and reduce the amount of material in the tiedown system.

In selecting cable size, the diameter was chosen in the same proportion to cable length as that on the 17 meter turbine. This yields a dynamically similar stiffness on top of the tower regardless of absolute rotor size.

Selecting the pretension is more complex. Pretension is required because of cable droop, which occurs in the downwind cable when the tower is loaded by aerodynamic blade forces. This droop drastically reduces the effective stiffness of the downwind cable and increases the possibility of a blade striking a cable. In the optimization model, the pretension is chosen so that the loss of downwind cable stiffness is less than 20% of the full, no-droop stiffness. The loading condition used for this requirement is a "normal" operating case, with the rotor at 150 fps tip speed in a 60 mph wind. Satisfying this stiffness requirement generally leads to cable droop displacements < 1% of the cable length.

Results for the cable pretension are shown in Fig. 3.11 for rotors with H/D's of 1.0 and 1.5. To satisfy the droop requirements, the pretension increases with rotor diameter to approximately the 2-1/3 power. Since cable strength grows with the square of the rotor diameter, there is some limiting size on tiedown systems designed to these pretension conditions. This effect is shown in Fig. 3.11 where the cable safety factor, defined as the ratio of cable ultimate strength to maximum working load, steadily decreases with increasing rotor diameter. However, for rotor diameters of < 300 ft., safety factors are still adequate.

Also shown in Fig. 3.11 is the first resonant frequency of the cable expressed as a multiple of the rotational frequency of the rotor. This curve is approximate in that the rotor frequency is estimated for normal operating conditions based on a 150 fps tip speed operating condition.

An actual turbine may differ in rotor speed from this estimate by 20% due to differences in rotor solidity or site wind characteristics. The fundamental excitation frequency into the cables is n per rev, where n is the number of blades. It is evident that $H/D = 1.5$ rotors with two blades will excite the cables above the first cable frequency. Alternatively, $H/D = 1.0$, two bladed systems provide excitation below the

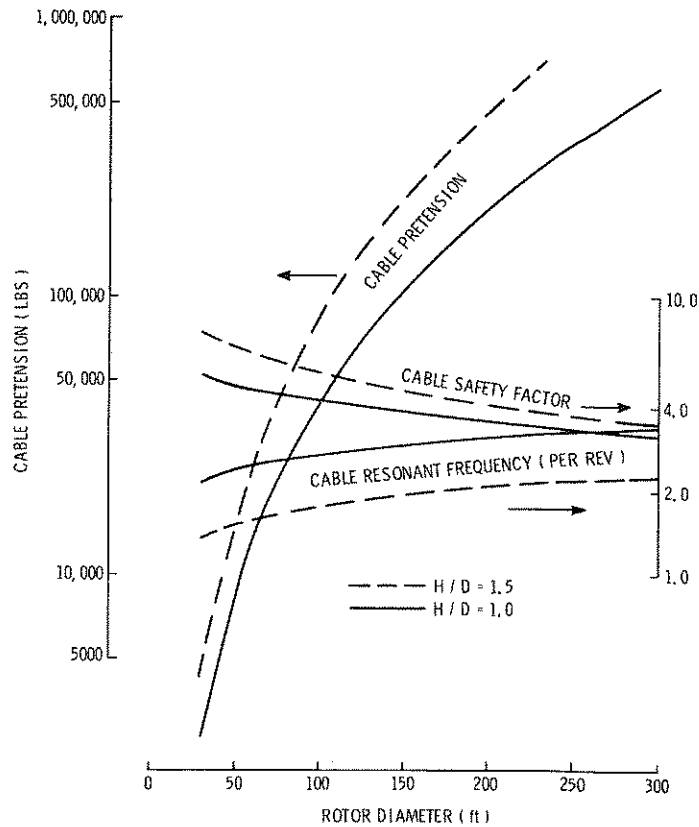


Figure 3.11 - Cable Pretension, Resonant Frequency, and Safety Factor as a Function of Rotor Diameter

first cable resonance. It is believed, based primarily on experience with the 17 meter rotor, that either case can produce acceptable cable performance although some fine tuning of the rotor rpm and/or cable tension may be required.

The prescribed cable tensions can have a considerable effect on system costs because of their influence on the tower sizing, rotor bearing requirements, and foundation loads. The pretension rules discussed have been successfully applied to the DOE/Sandia 17 meter rotor, but they are believed to be conservative. For example, the Canadian Magdalen Island rotor has roughly half the pretension indicated in Fig. 3.11. Future research directed toward establishing less conservative, lower tension design guidelines is advisable.

3.3 Component Cost and Weight Calculations

To minimize annual cost per unit of energy produced, costs of the major WECS subsystems are estimated in the optimization model. For the cost calculations to be useful for optimization purposes, it is necessary to estimate costs for a range of system parameters such as rotor diameter, operating speed, and rotor solidity.

Because of the large number of specially fabricated and purchased piece parts in a typical WECS, the task of cost estimating for a complete range of system possibilities is formidable. Fortunately, in the process of optimization it is not necessary to account for the cost of every system component. It is assumed that only the major system elements govern the optimization process. The major parts of the system included in the model are the rotor blades, tower, tiedowns, speed increaser, electrical system, and installation. It is believed that cost trade-offs between these items will dominate the selection of optima.

In conjunction with the cost calculations, estimates of component weights are also provided.

3.3.1 Rotor Blade Costs -- It is assumed that the blades are thin-walled, hollow extrusions with constant wall thickness. The blade construction process is as follows:

1. Straight sections are extruded as a single piece unless the chord length exceeds 24 inches. For blade chords above 24 inches, the cross section is constructed of multiple pieces, with no single piece exceeding 24 inches. These pieces are joined with a longitudinal weld under factory conditions.
2. The troposkien (Greek for "turning rope") shape of the blade²⁰ is approximated by straight and circular blade sections. The curved sections are to be bent at the factory, using an incremental bending process.
3. Transverse joints are used in the blade to permit shipping blade sections by conventional means. The shipment requirement is that formed blade sections can fit in a 60 x 12 x 12 ft. box. The transverse joints (if required) are constructed of hollow extrusions that fit inside the hollows of the blade. These joints are bolted together in the field.

The parts of this process that lead to recurring costs are raw materials, extrusion press time, joining of longitudinal and transverse sections, and bending the curved sections. Table 3.3 summarizes the rules used to determine these recurring costs in the blade cost model. Two major nonrecurring costs are also included in the model; these are the press setup charge (\$3000) and extrusion die cost (\$20,000). These nonrecurring costs are distributed over an assumed production run of 100 units and have relatively little impact on total blade costs.

Table 3.3
Blade Fabrication Cost Elements

Raw Material and Extrusion Press Time

\$2/lb of straight finished extrusions. Blade weight is calculated using the section of Fig. 3.7 with 20% additional weight for vertical section webs.

Longitudinal Joining of Sections with Chord Above 24 Inches

\$12/ft of finished weld.

Transverse Shipping Joints

Extruded joint inserts are used, assuming their weight per unit length is the same as blade sections. Length of inserts equal to two chord lengths per joint. Fabrication cost of \$2/lb assumed for joints.

Blade Forming of Curved Blade Sections

Incremental bending cost is taken to be proportional to blade length, based on 48 man-hours @ \$25/hr used for the curved blade spars on the DOE/Sandia 17 meter turbine.

The cost formulas are based primarily on discussion with the aluminum industry and our experience in past blade procurements. Of the costs accounted for, the curved section bending and longitudinal welding costs are the most uncertain. These costs are probably quite sensitive to the degree of automation associated with the processes. The costs in Table 3.3 are conservative estimates for nonautomated bending and welding methods.

Blade costs are calculated in the optimization model, given the geometrical parameters of chord, wall thickness (subject to structural constraints), rotor diameter, and rotor H/D ratio. An option to include blade support struts as part of the blade cost is available. These supports are assumed to have the same cross sections as the other blade sections so that their cost is accounted for as additional blade length.

Figure 3.12 shows typical single blade costs as a function of rotor diameter. This particular figure is for a fixed rotor solidity (0.135) and wall thickness-to-chord ratio (0.006). Discontinuities in the cost are due to the requirement of multiple piece extrusions when the chord is greater than 24 inches. Also shown is the blade weight.

Figure 3.13 indicates the fraction of total blade costs devoted, respectively, to raw extrusions and postextrusion work such as bending the curved sections and making longitudinal welds. Note that the raw extrusion cost dominates the larger systems.

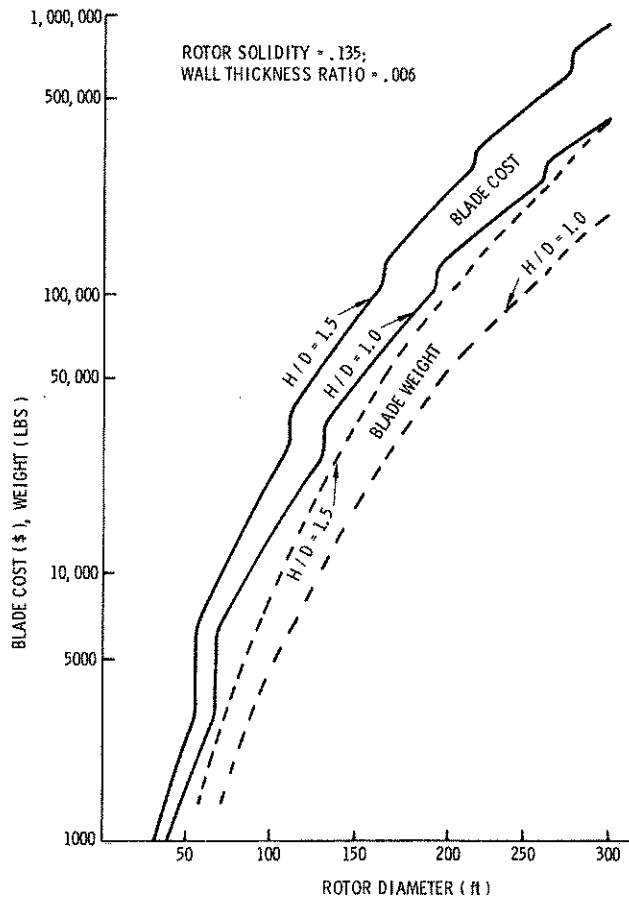
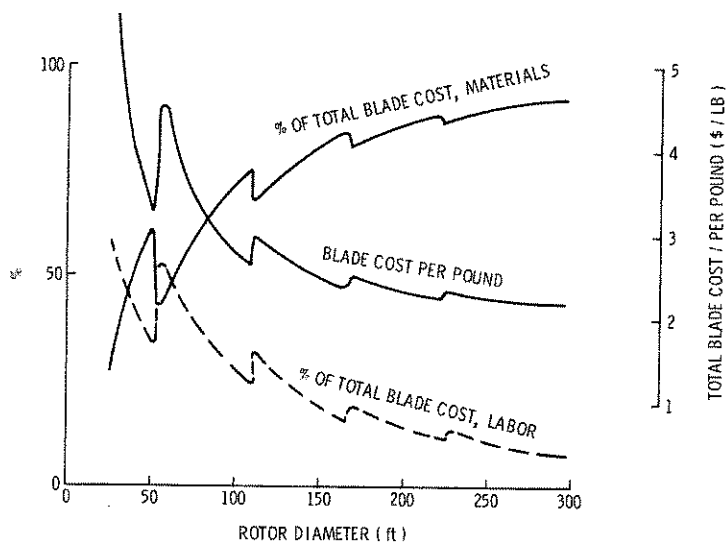


Figure 3.12 - Single Blade Cost and Weight as a Function of Rotor Diameter

This effect is also shown in Fig. 3.13, where the cost per pound of finished blade approaches \$2 as diameter increases.

3.3.2 Tiedown and Tower Costs -- Both these costs are estimated from the weights of relevant components.

Tiedown weights are calculated from the structurally constrained cable diameter and its weight. The tiedown system cost is taken at \$2.50/lb of cable. This per-pound cost is high for standard galvanized bridge strand (\$1.00-1.50/lb), but the conservatism is appropriate since the weight of cable attachment hardware has not been included.



H / D = 1.5

Figure 3.13 - Finished Blade Cost per Pound and Percentage of Costs for Labor and Materials. H/D = 1.5 Rotor.

The tower, made entirely of steel, consists primarily of large diameter, thin-walled, spiral welded tubing between the blade attachment fittings. The diameter and wall thickness of this tube are determined structurally (see Section 3.2.2). The tower also has transition pieces to mate the much smaller diameters of the tiedown bearing and transmission input shaft to the central tube. The weight of these items is estimated assuming the transition to occur in one tube diameter. Blade attachment fittings are also part of the tower. Fitting weights are estimated assuming the volume per fitting is equal to the blade interior volume for a single chord length.

From the sum of these weights, the tower cost is calculated using \$1.50/lb, a typical selling price for mild steel components of this type.

The weight and hence the cost of the tower and tiedown systems are affected by the blade ground clearance. A minimum possible ground clearance is dictated by the height of the transmission and the length of the tower-to-transmission transition piece (see Section 4.2.4). If the specified ground clearance is greater than this minimum, length is added to the thin-walled, tubular sections. This increased length affects the tiedown length, cable diameter, cable pretension, and tower axial load. This in turn affects the tube dimensions and weight through the structural constraints. The net effect is an increase in tower and tiedown costs, depending on the ground

clearance. This effect is included in the optimization model so that the impact of ground clearance could be investigated.

3.3.3 Transmission Costs -- A gear-type compact gearbox is used to convert the relatively slow speed output of the rotor to a high speed (1800 rpm) shaft suitable for use with standard electrical generators. A study by Stearns-Roger, Inc.¹⁰ of drive train economics* is the main source for cost data used in the optimization model.

Figure 3.14 shows various gearbox costs as quoted by four vendors to Stearns-Roger.

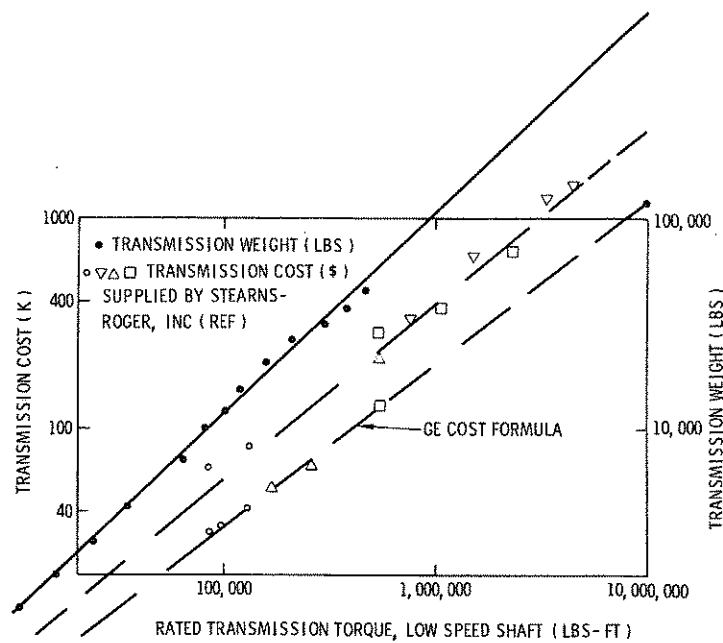


Figure 3.14 - Gearbox Cost and Weight as a Function of Rated Transmission Torque

There is considerable scatter in these data, indicating that the cost of a transmission greatly depends on the supplier selected. The lowest cost transmissions were used to generate a cost formula, because a wind turbine company in production presumably would seek out the least expensive supplier.

*The Stearns-Roger study considered other power conversion possibilities besides the compact gearbox/high speed generator. These include slow speed DC generators; belt or chain drives; and large diameter, exposed gear transmissions. The study concluded that the most economical concept with minimum development time is the compact gearbox directly coupled to a high speed generator.

A formula similar to one used in the GE conceptual design study on horizontal axis systems¹ is also shown on the figure:

$$C_{\text{trans}} = 3.2(\text{rated torque})^{0.8}$$

This formula is used in the optimization model, and it appears to be reasonable for the lowest cost transmissions with peak torque ratings below 500,000 ft-lb. Caution is appropriate for very large transmissions (1,000,000 ft-lb and up), as the formula underpredicts the cost of such large transmissions.

Figure 3.14 also shows gearbox weight as a function of rated torque. These weights were obtained from a Philadelphia Gear catalog and should be representative of parallel shaft gearboxes since the materials and construction are similar. The overall cost per pound for these gearboxes is around \$3, using the above cost formula.

An important factor in determining drive train costs is the transmission service factor defined as the ratio of the transmission torque capacity to the expected maximum torque transmitted. Service factors greater than unity may be required on the WECS to ensure long transmission life in the presence of torque transients that exceed the expected maximum driveline torque; or service factors less than unity may be possible because the system spends only a fraction of total operating time at rated conditions. In most results presented in this volume, a service factor of 1 has been used, but a user option is available to change the service factor if desired.

3.3.4 Generator and Electrical Controls -- The electrical system consists of an 1800 rpm induction motor/generator with a fixed mechanical connection to the high speed shaft of the transmission.

The generator is also used as a motor to start the Darrieus rotor from rest. In the starting mode, a reduced voltage starter is required to avoid transmitting excessive torques through the drive train. This starting process is limited by the heating of the motor during startup. Stearns-Roger¹⁰ has shown that the process is feasible, with certain exceptions for very large rotors (diameters above 150 feet) operating at relatively high rpm. Modifications to the starting system, such as mechanical clutches and/or heavy duty electrical equipment, may be required in these special cases. In assessing electrical system costs, these special cases are not considered. As the electrical and starting system is a very small fraction of total system cost on large rotors, this simplification is not particularly significant.

Typical list prices for 1800 rpm synchronous and induction generators are shown in Fig. 3.15. A formula used by Kaman² for generator cost is also shown. As is the case for transmission costs, there is considerable scatter in these data. List prices

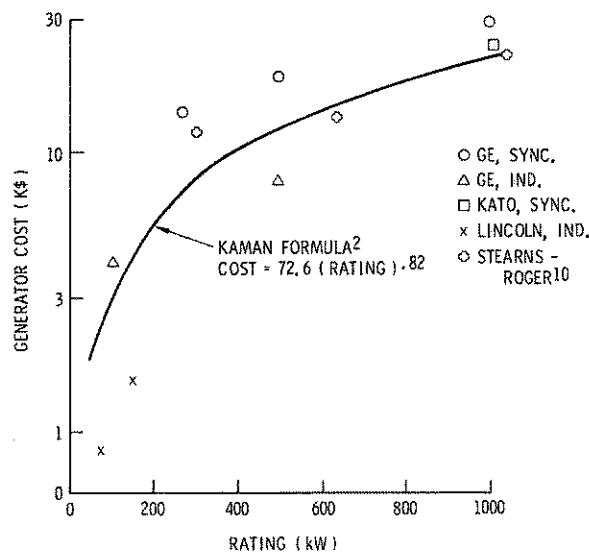


Figure 3.15 - Costs of Synchronous and Induction Generators

for similar generators may vary by a factor of two, depending on the supplier. The Kaman formula does appear to be reasonably representative, however, and therefore it is used in the optimization model.

The dominant cost items necessary to connect the generator to the utility line are a 1) three phase circuit breaker, 2) reduced voltage starter, and 3) transformer (optional). The transformer option depends on the available utility line voltage and the economic tradeoff of the cost of high voltage electrical equipment vs a transformer and lower voltage equipment.

The cost of controls is quite sensitive to the available utility line voltage. Two user-selected possibilities are included in this study: 460 V for systems below 300 kW, or 4160 V for all sizes. In the 460 V case, no transformer is used and all controls operate at 460 V. In the 4160 V case, either 4160 V controls (no transformer), or 460 V controls (with transformer) are used, the choice depending on relative costs.

Figure 3.16 shows the cost of the controls for both the 4160 V and 460 V cases. Sources of individual cost points on these curves are indicated. The solid lines are the approximations used in the optimization model. The break in the 4160 V cost curve is due to a switch to a transformer at power levels below 600 hp. The controls cost is added to the generator cost to obtain a total electrical system cost.

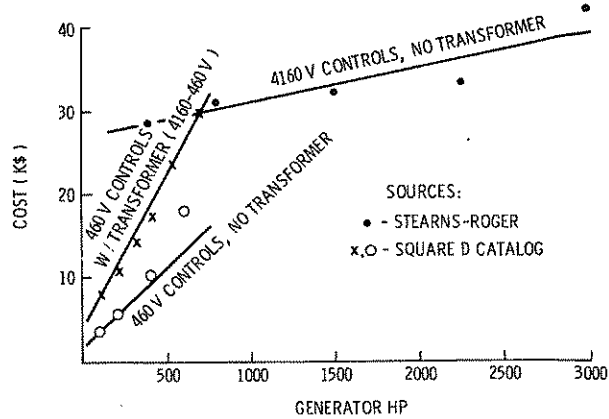


Figure 3.16 - Cost of Electrical Controls

It is possible to input a service factor on the electrical system for assessing the costs of over- or under-rated systems. This is a practical consideration for analyzing specific designs, since using shelf electrical equipment to the turbine usually requires some mismatch in rotor output and generator rating.

3.3.5 Installation Costs -- Installation costs cover the labor, material, and equipment needed for foundation construction, assembly, and erection of the turbine.

Foundation costs are estimated from the volume of concrete required for the rotor base pad and the three tiedown footings. The total volume of the three tiedown footings is estimated to be equal to the rotor base volume. The concrete volume required was scaled from the minimum foundation requirements on the DOE/Sandia 17 meter rotor as the cube of the rotor height. Costs of concrete foundation work are as follows:

<u>Concrete Work</u>	<u>Cost (\$)</u>	
Forming	= 1.34/ft ²	(labor and material)
Excavating	= 0.0838/ft ³	(labor and equipment)
Finishing	= 2.01/ft ³	(labor and material)
Reinforcing	= 0.84/ft ³	(labor and material)

The assembly and erection assume the following labor and equipment requirements:

<u>Labor</u>	<u>Number of Days</u>	<u>Cost per Worker (\$/hr)</u>
1 Foreman	N*	19.96
1 Forklift Operator	N	15.86
2 Crane Operators	3	18.14
4 Laborers	N	12.54
2 Electricians	4	18.53
2 Surveyors	4	17.00
1 Trencher Operator	1	15.86
<u>Equipment</u>		
2 Light Trucks	N	63.0 (\$/day)
1 Forklift	N	155.0 (\$/day)
1 Trencher	1	76.0 (\$/day)
2 Cranes	3	Varies with rotor size (Approximately \$2400/day for 100 ft. diameter)

*N = variable number of days

The number of days, N, is the critical parameter in the assembly. N is assumed to be 7 days for a turbine diameter of 60 ft. and is scaled up linearly with diameter for larger rotors.

Electricians, surveyors, and crane operators are viewed as being needed a set number of days regardless of turbine size above 60 ft. The cranes are needed 3 days, and a cost formula based upon turbine size was developed using actual local crane rental data.

Turbines having diameters < 60 ft. will not require as much manpower or equipment as outlined above. For turbines < 20 ft. in diameter, a fixed assembly cost of \$1000 is assumed, with the assembly costs increasing linearly between 20 ft. to the 60 ft. in diameter full crew assembly cost.

A fencing cost is also included in the installation. The fence simply surrounds the turbine base and its cost is scaled linearly with turbine diameter.

Total costs of foundations and erection are shown in Fig. 3.17. The rapid growth of the installation cost on large rotors is due primarily to the growth in foundation volume. The H/D = 1.5 rotor installation costs are substantially higher because of the larger foundations and cranes required. This difference decreases on small rotors, where labor charges, which are relatively insensitive to height, dominate.

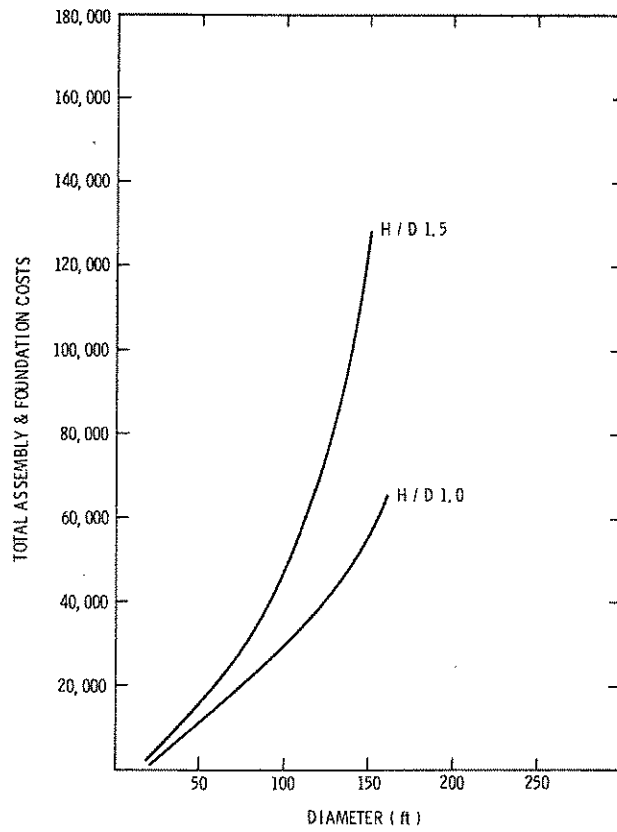


Figure 3.17 - Installation and Assembly Costs as a Function of Rotor Diameter

4. Economic Optimization Model Results

The major results obtained from application of the optimization model are the prediction of the cost of energy and net energy production of optimized systems, identification of optimum design parameters, and a summary of the system parameters selected for the point designs. Each area will be discussed separately.

Interpretation of absolute costs provided in this chapter should be cautious in view of the approximations built into the model. The reader is advised to consult Volume IV of this study where the costs of each point design are analyzed in substantially greater detail. The discussion here is restricted to relative cost issues and the interpretation of the economic trends observed.

4.1 Cost per Kilowatt-Hour and Performance of Optimized Systems

The predicted installed system cost per kilowatt-hour is governed by the ground rules discussed in Section 1. Probably the most significant rule is the 15% annual charge that is assumed to be the total cost to the owner for financing and operating the system. Converting presented cost per kilowatt-hour to any other annual charge rate is easily done by multiplying these results by the ratio of the new charge rate to 15%.

Table 4.1 summarizes typical properties of the optimized systems. The rationale leading to these selections is discussed in Section 4.2.

Table 4.1
Typical Properties of Optimized Systems
(15 mph Median Windspeed Distribution)

Rotor	H/D = 1.5, two blades, unstrutted (struts may be desirable for diameters above 150').
Solidity	Ranges between .12 and .14 depending on rotor diameter.
Rated Windspeed	Approximately 30 mph @ 30' reference height.
Cut-In Windspeed	Approximately 10-12 mph @ 30' reference height.
Plant Factor	From 20-25%, depending on rotor size.
Rotor Ground Clearance	As low as possible, with enough room for drive train placement except for smaller rotors (< 30' diameter) where a 10-20' clearance is advantageous.

In what follows, results are given for the cost of energy as a function of system size, performance as a function of system size, the effects of siting (meteorology) on cost of energy, and discussion of cost of energy sensitivity to possible errors and omissions in the optimization model.

4.1.1 Cost of Energy as a Function of System Size -- The cost of energy vs rotor diameter for optimized systems is summarized in Fig. 4.1. One significant feature of

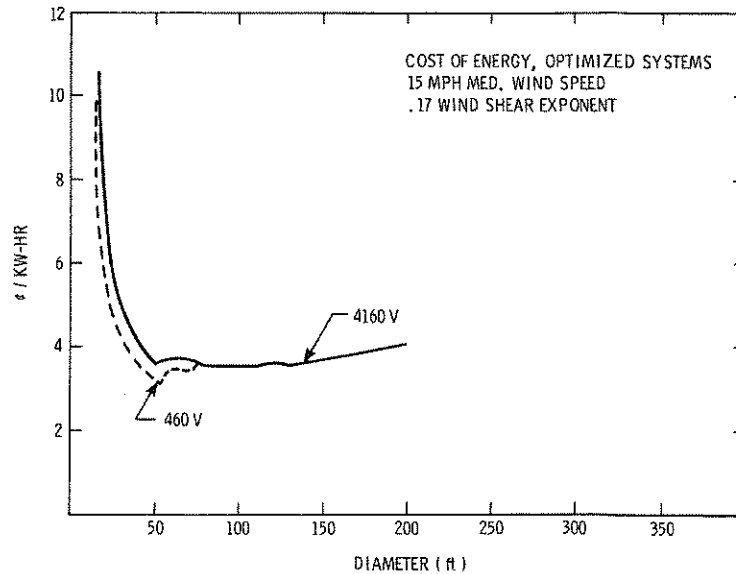


Figure 4.1 - Electrical Energy Costs for Optimized Systems from Version 16 of the Optimization Model

this curve is the lack of cost of energy sensitivity over a relatively wide range of rotor diameters, from 50 to 150 ft. in diameter. This corresponds to power ratings from ~ 100 to 1500 kW (see Section 4.1.2). On either side of this range, the model indicates a definite trend towards less cost-effective systems.

Another apparent feature of the cost curves is a lack of smoothness, an effect due primarily to discrete changes in blade costs that occur as the blade chord and length increase (see Section 3.3.1). Larger blades require more joints as fabrication and/or shipping constraints are encountered, and the addition of joints increases the cost in discrete jumps.

Identifying the cost drivers on the WECS gives some insight as to the nature of the cost of energy curve. Percentages of the total system cost of the rotor (blades and tower), tiedowns, transmission, electrical components, and field work (foundation, assembly, and erection) are shown in Fig. 4.2 as a function of rotor diameter. This curve demonstrates a fundamental difference between large and small systems: the electrical system dominates for small systems, whereas structural hardware, particularly the rotor, dominates the larger systems. This effect is explained as follows.

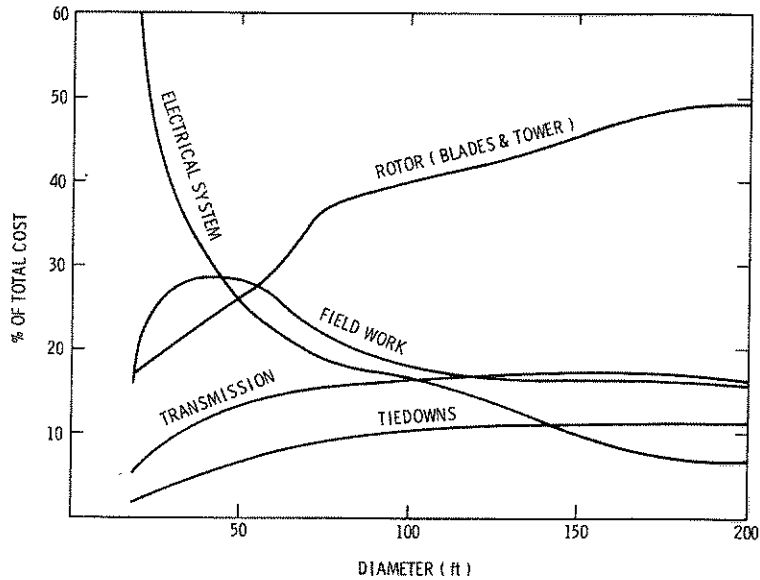


Figure 4.2 - Distribution of Subsystem Costs for Optimized Designs

Electrical system costs are roughly proportional to the peak power rating of the system which varies with approximately the square of the rotor diameter. Alternatively, structural hardware cost tends to be proportional to its volume, which varies with nearly the cube of the rotor diameter for structures designed to the same level of structural performance. (See, for example, Fig. 3.12 for blade weight and cost variation with rotor size.) Of course, actual relative growth rates of subsystem cost and energy collection capacity as rotor size increases are not such simple proportions due to wind shear effects and because component costs include labor and handling in addition to material (volume dependent) costs. Nevertheless, the qualitative source of the difference in electrical and structural component cost growth rates offered by the simple scaling argument is quite reasonable and leads to the behavior of Fig. 4.2.

The tendency of the large systems above 150 ft. in diameter to have a higher cost of energy is produced by the same effect. The incremental increase in cost of the structural components exceeds the incremental increase in energy collected by the system. Figure 4.3 shows the energy collected per pound of total system weight (excluding foundations) as a function of rotor diameter. The kW-hr per pound of system weight continually decreases and for systems large enough to be dominated by material costs, this effect will eventually cause an increase in the cost of energy. In this economic model, the declining kW-hr/lb tends to adversely affect the system cost of

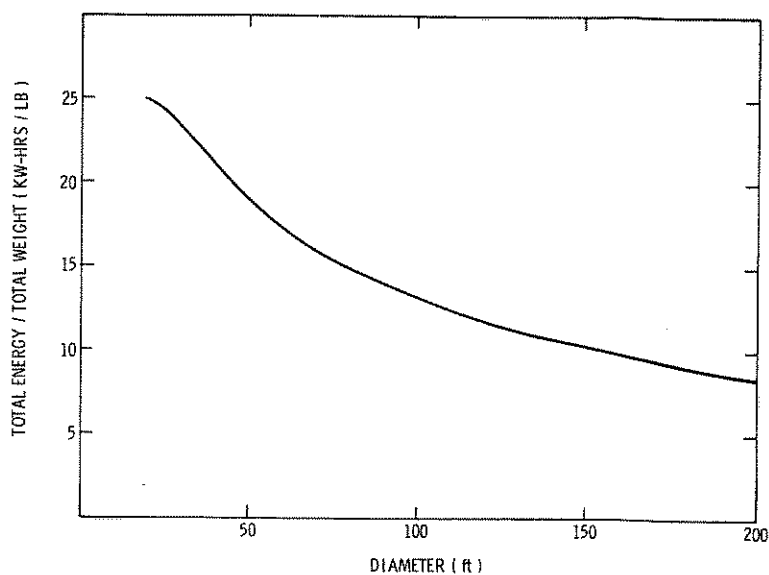


Figure 4.3 - Energy Collected per Unit of System Weight Tends to Decrease with System Size

energy at diameters above 150 ft. However, there are economic and performance factors that can substantially change this breakover diameter. Several factors of this type will be discussed in Sections 4.1.3 and 4.1.4.

The smaller systems (less than 50 ft. in diameter), while benefitting from a low system weight per unit of energy collected, are costly because of the high cost of the electrical components. Incidentally, electrical system cost depends significantly on the utility grid voltage available (see Section 3.3.4). The solid curve in Fig. 4.1 is for a 4160 V system, which generally requires a transformer. The dotted line is for a lower voltage (460 V) connection that eliminates the transformer and noticeably reduces the cost of energy.

4.1.2 Annual Performance and Total Cost of Optimized Systems -- Figure 4.4 summarizes the performance and total cost for optimized systems. Two performance measures are shown, the average power and the rated power. The average power is defined as the total annual energy collected divided by the total time in a year, 8760 hours. Rated power, a more frequently used measure of WECS size, is the peak output of the system. The rated power for a Darrieus system optimized for a 15 mph median wind-speed distribution generally occurs at windspeeds above 30 mph (30' reference height). The rated power varies strongly with small perturbations in synchronous rotor rpm (see Section 4.2.1). The tradition of rated power as a measure of system size should

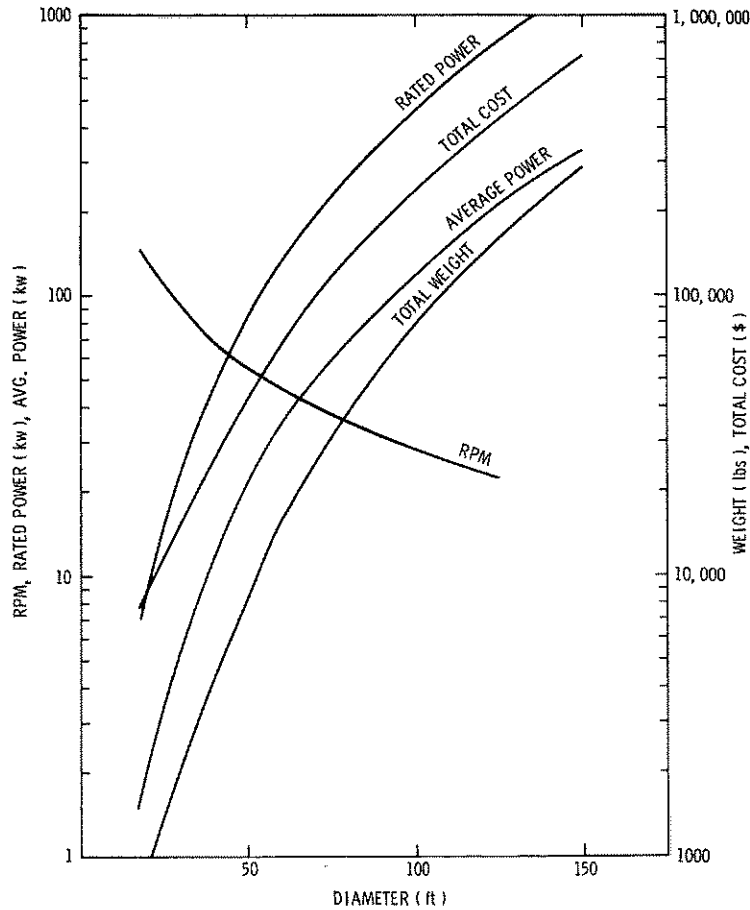


Figure 4.4 - System Performance Parameters as a Function of Rotor Size

be used cautiously in view of this sensitivity. The average power and cost of energy are much less sensitive to perturbations in the optimization process.

WECS performance is proportional to ambient air density. A sea level air density (0.076 lb-m/ft^3) has been used throughout this study. The effect on performance at sites with different density may be obtained by scaling the performance in direct proportion to the air density.

Rated and average power levels increase more rapidly than in direct proportion to the rotor area. This is shown in Fig. 4.5, where annual kilowatt-hours per square foot of rotor area are given as a function of rotor diameter. The increased utilization of the rotor as diameter (and height) increase is due to the wind shear effect.

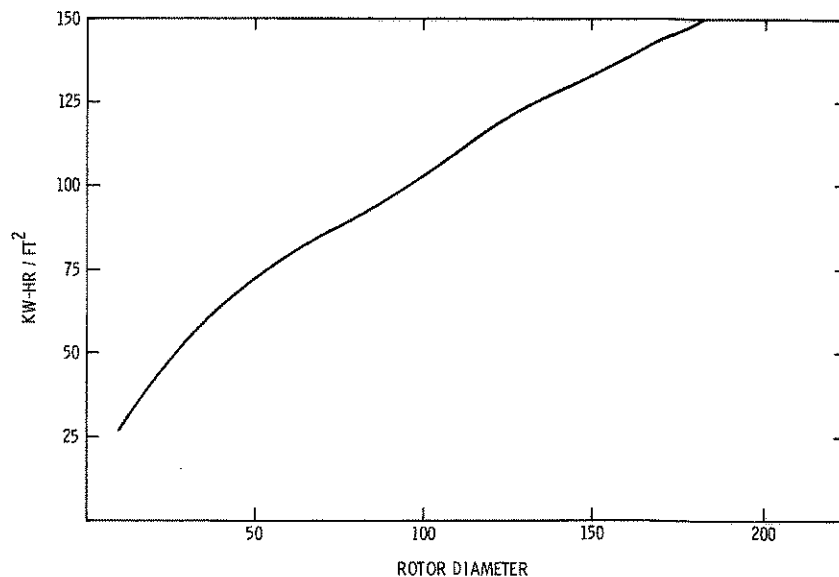


Figure 4.5 - Specific Rotor Performance (Annual Energy Collected per Unit of Rotor Area) Increases with Rotor Size due to Wind Shear. A Wind Exponent of .17 was used in this Figure.

The total weight of the system (excluding foundations), also shown in Fig. 4.4, grows roughly with the cube of the rotor diameter. This characteristic seems inevitable when comparing different size rotors designed to the same set of structural performance criteria.

4.1.3 Meteorological Effects on System Cost of Energy - Meteorological variables considered in this model are the median windspeed and the wind shear exponent (see Section 3.1.3).

Figure 4.6 shows the effect of windspeed distribution on the cost of energy, using the 12, 15, and 18 mph median windspeed distribution of Fig. 3.5. The solid lines represent optimized systems for each distribution. Costs associated with the different drive train ratings for each distribution are accounted for, but the tower, tiedown, and blade elements are assumed identical at all three sites. Since the tower, blades, and tiedowns are sized for the 15 mph distribution, this assumption is conservative for the 12 mph case and optimistic for the 18 mph case. The dotted lines on Fig. 4.6 are the cost of energy for systems operating at the same rotor rpm (and drive train ratings) as the 15 mph system. Such systems, although not optimized, are structurally

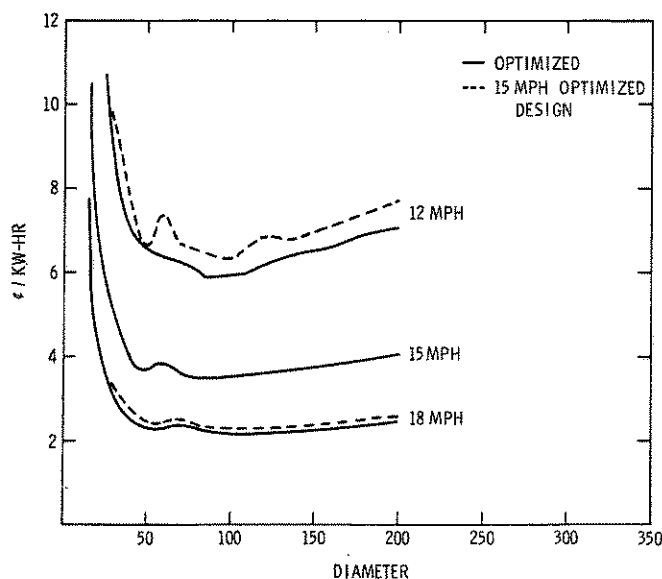


Figure 4.6 - The Effect of Median Windspeed on System Cost of Energy

sound as the aerodynamic and centrifugal loadings are dependent primarily on the rotor rpm. These "nonoptimized" systems represent an upper bound on the cost of energy at the 12 and 18 mph sites.

The effect of wind shear exponent is shown in Fig. 4.7 for the range of exponents from 0.1 to 0.24. Cost-effectiveness of large systems is clearly quite sensitive to the wind shear exponent. Figure 4.7 demonstrates the importance of accurately determining wind shear effects in siting larger systems.

4.1.4 Sensitivity of Cost of Energy Results to Changes in Cost Formulation --

While it is not possible to consider the effect on system cost of energy to all possible variations in the economic model formulation, a few general observations are possible. The perturbations in the model considered in this section are 1) uniform percentage change in the cost of all components, 2) a uniform fixed cost addition, 3) a cost change in a few (but not all) components, and 4) changes in the drive train service factor.

A uniform percentage increase in the cost of all components could occur due to, say, an unaccounted-for seller's markup. Such a change will not affect any trends observed and will simply change the cost of energy in proportion to the markup for all systems discussed. The effect is identical in consequence to an increase in the annual charge rate.

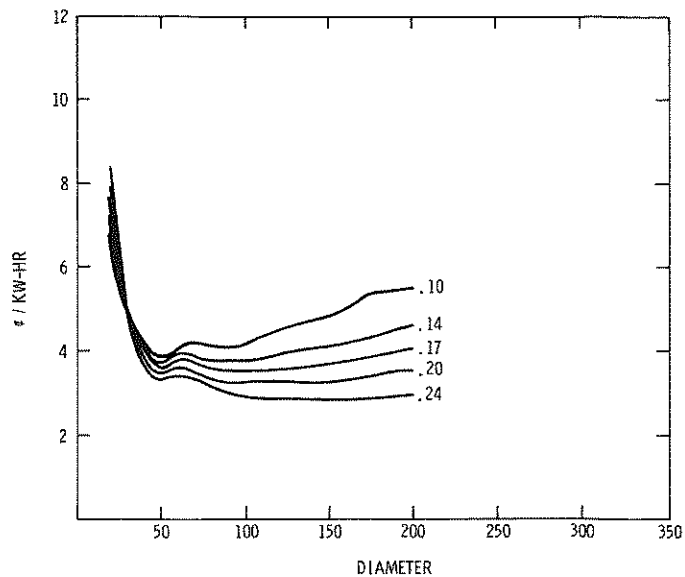


Figure 4.7 - Cost of Energy for Wind Shear Exponents from .1 to .24, 15 mph Median Windspeed Distribution

Fixed or nearly fixed costs are costs that vary none or little with the overall size of the system constructed. Such costs can occur from factory or distribution overheads associated with a wind turbine business. Operation and maintenance can also have fixed cost components. If large enough, these fixed costs can change overall trends in energy cost vs rotor size, as demonstrated in Fig. 4.8. The intrusion of fixed costs, even as low as \$10 K, can shift the favor toward larger systems. The selection of the best turbine should therefore be accompanied by an assessment of any fixed costs that may not be accounted for adequately in the optimization model cost formulas.

Cost adjustments on individual components of the system may be required because of new technologies or because of errors in the cost formulation presented here. The impact of such adjustments on total system costs can be estimated using the component percentage curves shown earlier (Fig. 4.2). Obviously, cost changes in items representing a small (large) fraction of total system cost will have a small (large) effect on the cost of energy.

Variations in transmission and generator service factors can affect energy cost through changes in drive train cost and efficiency. The minimum service factors possible in a WECS are uncertain because of ignorance of the magnitude and frequency of torque transients and the effect of such transients on transmission and generator life. Figure 4.9 shows cost of energy and average output power relative to service

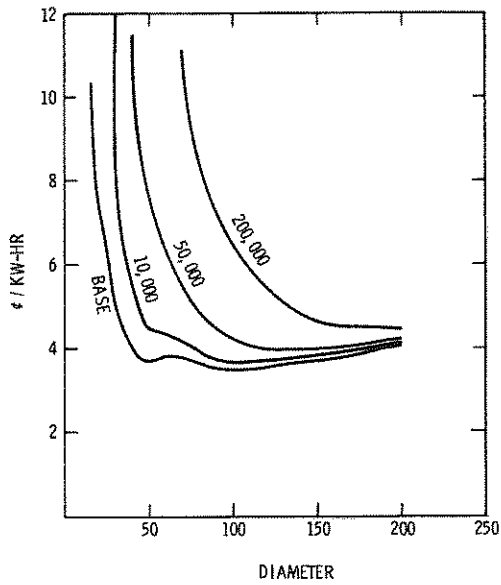


Figure 4.8 - The Influence of Fixed Capital Costs on the Cost of Energy

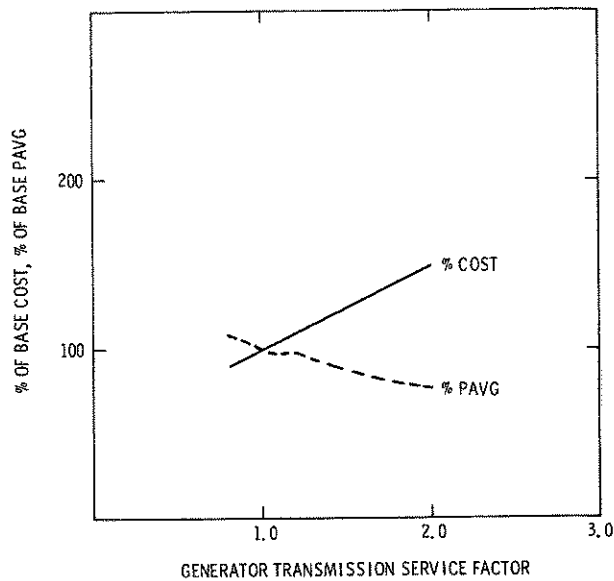


Figure 4.9 - Percentage of Base (Service Factor - 1.0) Cost of Energy and Average Annual Energy (PAVG) Realized for Various Generator-Transmission Service Factors. Results are for a 100 ft. Diameter Rotor.

factor 1.0 realized at service factors between 0.8 and 2.0. Evidently, using arbitrarily large service factors to cover drive train life uncertainties can be expensive. It is important that the minimum possible service factor be achieved through reduction of torque transients and/or by sufficient understanding of the effect of such transients on the life of the drive train to avoid unnecessary overdesign.

4.2 Identification of Optimum Design Parameters

Design parameters that are varied in the optimization process are the rotor diameter, rpm, solidity, number of blades, height-to-diameter ratio, and ground clearance. The effect of all these variables, except for rotor diameter, which was discussed in Section 4.1.1, will be discussed separately.

4.2.1 Rotor RPM -- For a given rotor configuration, the rotor rpm affects most overall system performance characteristics, such as the rated power, rated windspeed, and annual energy production. This differs from conventional horizontal axis systems where two variables govern the system performance; namely, rotor rpm and the pitch control criterion. VAWT power is controlled in high winds solely through the aerodynamic stalling characteristics of the blades.⁴ The "rated" windspeed at which this stall occurs depends only on the rotor rpm.

The effect of rotor rpm on system performance and cost is shown in Fig. 4.10.

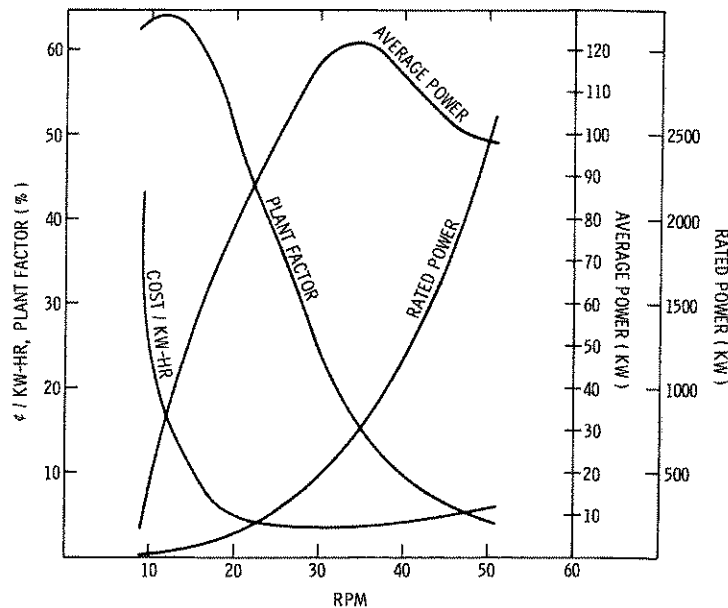


Figure 4.10 - System Performance as a Function of Rotor RPM

This particular example is for a 100 ft. diameter rotor with a H/D of 1.5. An optimum rpm in terms of the cost per kilowatt-hour is evident. At rotor speeds above the optimum, the rated power is high and plant factor* low. This produces high transmission and generator costs, and low overall mechanical-to-electrical conversion efficiency because the generator and transmission operate predominantly at fractional loads. These effects eventually cause the cost of energy to increase with increasing rpm. At rpm's below the optimum, the plant factors are much higher, but the rotor spends more time in the stalled condition, which reduces the aerodynamic energy collected.

It is noteworthy that the cost of energy reaches a very broad minimum, indicating that the rpm may be varied somewhat without significantly affecting energy cost. Alternatively, the rated power varies strongly with rpm. This effect permits some "tuning" of the rotor to be compatible with the specifications of available transmissions or generators and also to avoid rotor resonances.

The rated windspeed (not shown in Fig. 4.10) is directly proportional to the rpm and is approximately 30 mph (30' reference height) at the optimum rpm. This relatively high rated speed leads to the low plant factors (approximately 25%) at optimum rpm. If desired, the plant factor may be increased to over 50% by reducing the rotor rpm, though this will be at the expense of annual energy production (as reflected by the annual average system power), and the cost of energy will increase.

The results of Fig. 4.10 were obtained for the 15 mph median windspeed distribution of Fig. 3.5. Optimum rpm varies roughly in direct proportion to median windspeed for other windspeed distributions.

4.2.2 Rotor Solidity and Number of Blades -- The solidity of the rotor and the number of blades determine the blade chord. The minimum structurally possible wall thickness (see Section 3.2.1) is used for any particular choice of blade chord. The energy cost for a 100 x 150 ft. rotor as a function of solidity is shown in Fig. 4.11 for two- and three-bladed rotors. Both cases demonstrate an optimum solidity.

The cost of energy generally varies quite slowly with solidity, indicating no necessity to be precise about solidity selection. However, an important exception is indicated by the step changes in the cost of energy that occur at certain discrete solidities shown in Fig. 4.11. These steps are caused by a change in the number of extrusions required to construct the blade cross section. The necessity for additional pieces occurs at discrete chords corresponding to multiples of the maximum

*"Plant factor" is defined for these systems as the percentage ratio of the annual average power to the rated power.

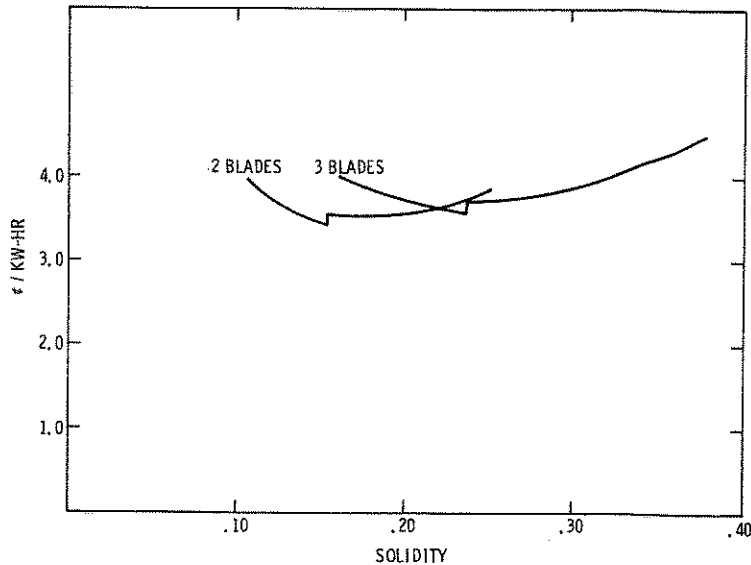


Figure 4.11 - The Effect of Solidity on Cost of Energy for Two- and Three-Bladed Rotors Without Support Struts

extrusion press size. These additional pieces require considerable additional labor and tooling costs (see Section 3.3.1). It is important, therefore, to select a solidity that avoids being close to the high side of such a step.

Several balancing effects are traded off to yield an optimum solidity. At low solidities, the blade costs are reduced and the rotor rpm increases, which reduces the speed increaser cost. But aerodynamic output is impaired at low solidities, which eventually causes the cost of energy to increase. At high solidities aerodynamic output is improved, but this benefit is offset by increased blade and transmission costs.

A three-bladed system optimizes at a higher solidity, with the minimum cost per unit of energy slightly higher than for the best two-bladed systems. Although the cost difference is small, the increased complexity of a three-bladed rotor provides additional incentive to use two-bladed rotors. But the economics indicate that should technical issues (such as torque ripple¹¹) increase the desirability of three-bladed designs, they can be obtained without prohibitive economic impact.

Figure 4.12 shows similar results with blade support struts included. These struts permit the use of thinner walled blades because of the strengthening effect of

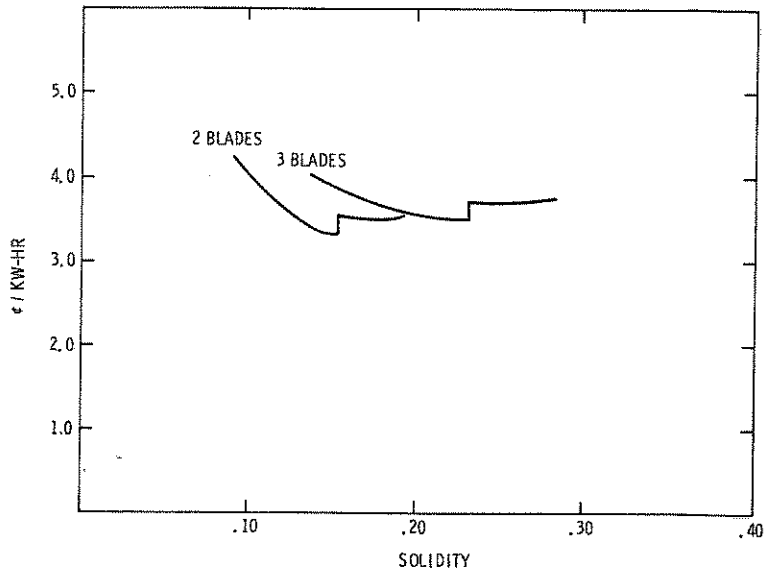


Figure 4.12 - The Effect of Solidity on Cost of Energy for Two- and Three-Bladed Rotors with Support Struts

the struts (see Section 3.2.1). The minimum cost strutted systems, after appropriate reduction of blade wall thickness, have approximately the same cost of energy as do unstrutted rotors. The simplicity of the unstrutted rotor favors its use, although struts may be desirable on very large systems (above 150 ft. in diameter) for the attenuation of gravity loads.

4.2.3 Rotor Height-to-Diameter Ratio -- The rotor height-to-diameter ratio is a fundamental design parameter that affects a variety of performance and cost issues. Figure 4.13 shows the effects on system cost of energy for a 40,000 ft.² rotor as a

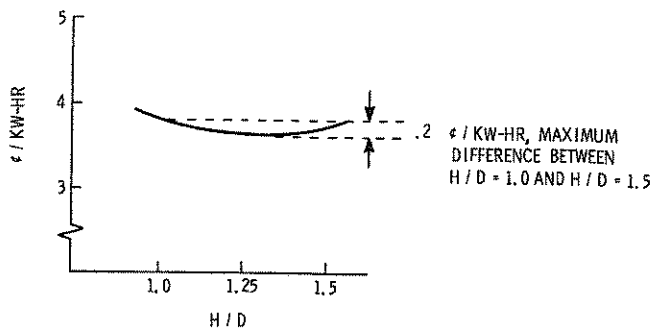


Figure 4.13 - The Effect on Cost of Energy of Rotor H/D, 40,000 ft.² Rotor.

function of the rotor height-to-diameter ratio. It is apparent that the optimum systems have $H/D \approx 1.25$.

For rotors with the same swept area, two major factors favor large height-to-diameter ratios. First, the overall height of the rotor is increased, which in conjunction with wind shear increases the energy available to the rotor. Secondly, an optimized Darrieus rotor tends to operate at roughly the same tip speed, independent of H/D . A large H/D rotor operates at a higher rpm for a given tip speed, and this reduces maximum drive train torque. The net effect is reduced transmission cost. Major disadvantages of large H/D are increased tower, tiedown, and installation costs due to the greater height of the rotor, and a gradual decrease in aerodynamic performance (optimum aerodynamic performance occurs near $H/D = 1.0$). These negative effects begin to dominate as H/D increases above 1.5.

The effect of reducing H/D is just the opposite. Tower, tiedown, and installation costs are reduced but transmission costs increase and wind shear benefits are reduced. The overall balancing of these advantages and disadvantages leads to the low ratio of system cost of energy sensitivity to H/D shown in Fig. 4.13. However, certain factors not accounted for in the optimization model have led to the choice on the point designs of the largest cost-effective H/D ; i.e., $H/D = 1.5$. These other factors are the improved tiedown clearance and reduced blade curvature associated with larger height-to-diameter ratios. It is believed that these factors will ease design, manufacture, and shipping of the rotor. However, should other technical or economic issues be discovered that favor lower H/D rotors, the use of rotors with height-to-diameter ratios as low as 1.0 should be possible without undue economic impact.

4.2.4 Rotor Ground Clearance -- The clearance between the lower blade attachment fittings and ground level is a factor which may be varied to some degree in the design process. The method considered here is to simply increase the tower length.

In considering variations in ground clearance, there is a minimum possible clearance which is required to clear the transmission, generator, and leave room for tower-to-transmission couplings. This minimum value will depend on the size of the machine and the specific nature of the design. The optimization model assumes a minimum 12 ft. clearance for a 100 ft. diameter rotor and scales this value in proportion to rotor diameter for other sizes. The minimum 12 ft. clearance is based on typical transmission and coupling dimensions for a 100 ft. rotor.

The fundamental tradeoff occurring upon addition of ground clearance is between increased energy collection from wind shear and increased cost in the tower and tiedowns (see Section 3.3.3). Figure 4.14 shows the cost of energy as a function of ground clearance for rotor sizes from 18 ft. to 100 ft. in diameter. The larger

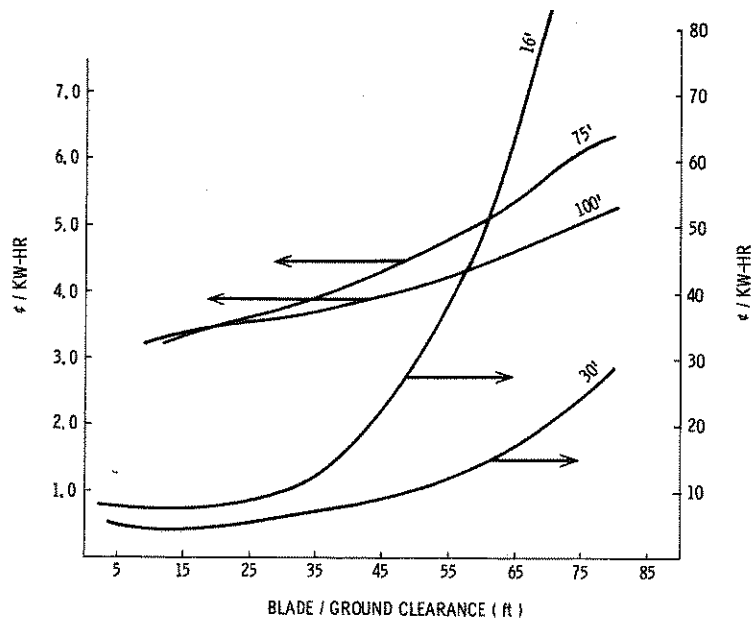


Figure 4.14 - The Effect of Rotor Ground Clearance on Cost of Energy

rotors (above 75 ft.) indicate a steady decrease in cost of energy as the clearance is reduced to the minimum value. The two smaller rotors show an optimum clearance in the range of 15 ft. All cases show a rather modest dependence of cost of energy to ground clearance.

The qualitative difference between large and small rotors regarding optimum ground clearance is because of the difference in cost of the tower and tiedowns relative to total system cost (Fig. 3.2). The total cost of smaller systems is dominated by electrical costs and so the increase in total cost due to a clearance increase above the minimum value is relatively unimportant. The opposite is true for larger systems.

The results given here only apply for a wind shear exponent of .17 and for the method of adjusting ground clearance by extending the tower. Naturally, systems at sites with different wind shear properties or with unique geological features may be more or less sensitive to the choice of ground clearance.

4.3 Specifications and Performance of the Point Designs

Six sets of system specifications have been developed for the point design process. These specifications cover a range of rotor diameters from 18 to 150 ft., corresponding to approximate power ratings from 10 to 1600 kW. The range of sizes is

intended to include the systems with the least cost of energy predicted by the optimization model. The larger and smaller systems in the range are on the higher portion of the $\phi/\text{kW-hr}$ curve (Fig. 4.1). This is intentional, so that the predicted trends toward increasing costs could be verified or modified based on the results of detailed economic analyses of the point designs.

The careful observer will note that some of the point design specifications differ from the optimum values presented in Section 4.2. These inconsistencies are caused by the fact that specifications were set with earlier versions of the economic model. This was unavoidable because the lead time necessary to complete the point designs required a commitment to the specifications while the optimization model continued to be refined. However, in presenting the model-predicted costs, weights, and performance of the point designs, the latest versions of the economic model are used. The deviation of specifications from current optima affects the cost of energy by less than 5%, a very small effect when considering the overall resolution of the model.

The six point designs are referred to by approximate peak power ratings (10, 30, 120, 200, 500, and 1600 kW). These ratings are rounded off considerably and the actual peak output power of each design may differ by as much as 20% from these nominal values.

The 10, 30, and 200 kW systems are unique in that an attempt was made to optimize the rotor diameter to a fixed blade chord (6", 11", and 29", respectively), rather than optimizing the chord for a fixed rotor diameter. The overall effect on optimized cost of energy due to this subtle difference in optimization is hardly detectable, but it does produce noticeable differences in the optimized specifications, particularly the rotor solidity. This difference should be taken into account when attempting to discern trends within the point design specifications.

The point design properties are summarized in the four following tables (4.2 - 4.5), with data on rotor geometry, system performance, predicted component weights, and predicted component costs.

Table 4.2
Rotor Geometry for the Point Designs

Nominal Rating (kw)	10	30	120	200	500	1600
Diameter x Height (ft)	18 x 27	30 x 45	55 x 83	75 x 120	100 x 150	150 x 225
Collection Area (ft ²)	324	900	3000	5600	10,000	22,500
Ground Clearance (ft)	10.	10.	10.	17.	13.	17.
Blade Chord (in)	6	11	24	29	43	64
Blade Wall Thickness (in)	.125	.22	.24	.25	.25	.38
Rotor Solidity	.104	.120	.135	.120	.134	.134
Tower Diameter (ft)	2.0	2.4	3.7	4.7	6.3	9.4
Tower Wall Thickness (in)	.032	.032	.060	.090	.140	.20
Tiedown Tension (lbs)	1700	5000	20,000	46,000	86,000	230,000
Number of Blades	2	2	2	2	2	2

Table 4.3
Performance Characteristics of the Point Designs
(15 mph Median Distribution)

Nominal Rating (kW)	10	30	120	200	500	1600
Actual Peak Output (kW)	8	26	116	226	531	1330
Rated Windspeed (mph), 30' Ref.	34	32	31	30	31	30
Annual Energy Collection (MW-hrs/yr)	13.7	51.6	246	490	1070	2950
Plant Factor (%)	19.3	22.3	24.0	24.4	22.6	24.9
Rated Rotor Torque (ft.-lb)	398	2260	17,600	45,200	136,000	497,000
Rotor RPM	163	95.0	52.0	40.1	31.1	21.0
Blade Reynolds Number (Millions)	.47	.89	1.8	2.3	3.6	5.5
Maximum Power Coefficient	.34	.37	.38	.37	.39	.39

All Results are for Sea Level Air Density
Performance Calculations from Version 16 of the Optimization Model

Table 4.4
 Predicted Component Weights (lbs) for the Point Designs

Nominal Rating (kW)	10	30	120	200	500	1600
Weights (lbs):						
Blades	138	857	3640	6630	16,300	72,600
Tower	368	1050	4890	13,900	27,400	101,000
Tiedowns	105	353	1710	4680	9300	31,400
Transmission	48	272	2110	5430	16,300	59,600
Generator	161	434	1420	2420	4800	9990
TOTAL	819	2970	13,800	33,000	74,000	275,000
Annual kW-hrs per Pound of System Weight (kW-hrs/lb)	16.4	17.2	17.7	14.6	14.1	10.6

Table 4.5
 Predicted Component Costs for the Point Designs

Nominal Rating (kW)	10	30	120	200	500	1600
Component Costs (\$):						
Blades	1180	3110	9120	21,300	47,200	160,000
Tower	635	1910	8260	22,500	46,500	176,000
Tiedowns	262	883	4290	11,700	23,800	78,500
Transmission	399	1570	8020	17,200	41,200	116,000
Generator and Controls	2650 (460 V)	3920 (460 V)	9180 (460 V)	22,600 (4160 V)	45,300 (4160 V)	67,300 (4160 V)
Field Erection and Foundations	1260	4630	15,100	26,400	44,300	119,000
TOTAL	6380	16,000	54,000	122,000	248,000	717,000
\$/kW-hr @ 15% Annual Charge	6.97	4.65	3.30	3.72	3.50	3.65

All Costs from Version 16 of the Optimization Model

References

1. "Design Study of Wind Turbines, 50 kW to 3000 kW for Electrical Utility Applications - Volume II, Analysis and Design," General Electric Co., December 1976, ERDA/NASA/9403-76/2, NASA CR-134935.
2. "Design Study of Wind Turbines, 50 kW to 3000 kW for Electric Utility Applications - Analysis and Design," Kaman Aerospace Corp., February 1976, DOE/NASA/9404-76/2, NASA CR-134937.
3. B. F. Blackwell, R. E. Sheldahl, L. V. Feltz, "Wind Tunnel Performance Data for the Darrieus Wind Turbine with NACA 0012 Blades," Sandia Laboratories Report, SAND76-0130, March 1977.
4. J. F. Banas, E. G. Kadlec, W. N. Sullivan, "Application of the Darrieus Vertical Axis Wind Turbine to Synchronous Electrical Power Generation," Sandia Laboratories Report, SAND75-0165, March 1975.
5. R. E. Sheldahl, B. F. Blackwell, "Free-Air Performance Tests of a 5 Meter Diameter Darrieus Turbine," Sandia Laboratories Report, SAND77-1063, December 1977.
6. M. H. Worstell, "Aerodynamic Performance of the 17 Meter Diameter Darrieus Wind Turbine," Sandia Laboratories Report, SAND78-1737, January 1979.
7. J. H. Van Sant, R. D. McConnell, "Results of Preliminary Evaluation Tests of a 230 kW Vertical Axis Wind Turbine," Paper E2, Proceedings of the Second International Symposium on Wind Energy Systems, October 3-6, 1978, Amsterdam, The Netherlands.
- ✓ 8. J. H. Strickland, "The Darrieus Turbine: A Performance Prediction Model Using Multiple Streamtubes," Sandia Laboratories Report, SAND75-0431, October 1975.
9. B. F. Blackwell, "Program DARTER," unpublished.
10. "Cost Study, Vertical Axis Wind Turbine Power Conversion Systems," Stearns-Roger Engineering Co., Report No. C-19561, September 1977.
11. R. C. Reuter, M. H. Worstell, "Torque Ripple in a Vertical Axis Wind Turbine," Sandia Laboratories Report, SAND78-0577, April 1978.
12. R. J. Templin, P. South, "Canadian Wind Energy Program," Vertical Axis Wind Turbine Technology Workshop, May 17-20, 1976, Sandia Laboratories Report, SAND76-5586.
- ✓ 13. R. J. Templin, "Aerodynamic Performance Theory for the NRC Vertical Axis Wind Turbine," NRC Technical Report LTR-LA-160, June 1974.
14. Kaman Aerospace Corporation, private communication.
15. W. N. Sullivan, "Preliminary Blade Strain Gage Data on the Sandia 17 Meter Vertical Axis Wind Turbine," Sandia Laboratories Report, SAND77-1176, December 1977.
16. L. I. Weingarten, D. W. Lobitz, "Blade Structural Analysis," Vertical Axis Wind Turbine Technology Workshop, May 17-20, 1976, Sandia Laboratories Report, SAND76-5586.
- ✓ 17. W. N. Sullivan, "Structural Loads for the 17-m Darrieus Turbine," Vertical Axis Wind Turbine Technology Workshop, May 17-20, 1976, Sandia Laboratories Report, SAND76-5586.

18. R. C. Reuter, Jr., "Vertical Axis Wind Turbine Tiedown Design with an Example," Sandia Laboratories Report, SAND77-1919, December 1977.
19. R. C. Reuter, Jr., "Tiedown Cable Selection and Initial Tensioning for the Sandia 17 Meter Vertical Axis Wind Turbine," Sandia Laboratories Report, SAND76-0616, February 1977.
20. B. F. Blackwell, G. E. Reis, "Blade Shape for a Troposkien Type of Vertical Axis Wind Turbine," Sandia Laboratories Report, SLA-74-0154, April 1974.

GLOSSARY OF TERMS

1. System Components and Specifications
2. Rotor Geometry
3. Meteorological Factors
4. Aerodynamic and System Performance
5. Economic Factors

1. System Components and Specifications

Tower	--	The blade-supporting vertical rotating structure with associated bearings, blade attachment hardware, and tiedown connection fittings. Some units also have lightning protection devices and structures (base tower) to support the lower bearing.
Tiedowns	--	Subsystem for supporting the upper tower bearings including cable guys, cable terminations, and any tensioning hardware.
Rotor	--	Subsystem consisting of all low speed rotating parts, i.e.; tower, blades, and low speed shafts.
Drive Train	--	Subsystem consisting of all rotating components except the rotor.
Transmission	--	Speed increasing gearbox between the low speed rotor shaft and the high speed generator shaft.
Generator	--	Synchronous or induction machine to convert high speed shaft output of the transmission to AC electrical power.
Generator and Transmission Ratings	--	The maximum continuous duty power levels which can be transmitted by the generator and transmission.
System Power Rating	--	The maximum electrical output power expected from the system.
Generator and Transmission Service Factors	--	The ratio of continuous duty power ratings to the maximum expected output power from the system.
Generator and Transmission Efficiencies	--	The ratio of output power to input power.
Generator and Transmission Losses	--	The difference between output power and input power.
Electrical Controls	--	All electrical hardware required to connect the output of the generator to the utility grid and provide manual control of the system. Includes any electrical hardware required for starting the rotor.
Automatic Controls	--	All electrical or mechanical hardware required to provide unattended, automatic operations. Includes anemometry and measurement transducers as required.

2. Rotor Geometry

Rotor Diameter	--	Twice the maximum horizontal distance from the axis of rotation to the blade.
Rotor Height-to-Diameter Ratio (H/D)	--	The vertical distance between the upper and lower blade-to-tower attachments divided by rotor diameter.
Rotor Ground Clearance	--	The vertical distance between the lower blade attachment and ground level.
Rotor Centerline	--	A horizontal line, centered between the upper and lower blade attachment fittings.
Rotor Area (A)	--	Twice the area enclosed by one blade and the axis of rotation.
Blade Length	--	Total distance along the blade between the upper and lower blade attachments.
Blade Chord (C)	--	Straight-line distance between the blade cross-section leading and trailing edges.
Rotor Solidity (σ)	--	Total blade area (blade length x chord x number of blades) divided by rotor area.

3. Meteorological Factors

Annual Windspeed Distribution	--	A probabalistic distribution of windspeeds expected over a year at a particular site.
Annual Windspeed Duration Curve	--	A curve of windspeed vs. time indicating the amount of time in a typical year each windspeed is exceeded.
Median Annual Windspeed	--	That windspeed which is exceeded exactly half the time in a year.
Mean Annual Windspeed	--	The average of all windspeeds occurring annually.
Wind Shear	--	The tendency of windspeed to increase with distance above the ground.
Reference Height (H_{REF})	--	A specified measurement height associated with site wind statistical data. H_{REF} is taken to be 30 feet throughout this study.
Wind Shear Exponent (XPON)	--	Exponent used in the wind shear correction formula, $V_X = V_{REF} \left(\frac{X}{H_{REF}} \right)^{XPON}$; V_X is the windspeed at height X, V_{REF} is the windspeed at the reference height.

4. Aerodynamic and System Performance

Rotor RPM (RPM)	--	Rotor turning speed in revolutions per minute.
Rotor Rotational Speed (ω)	--	Rotor turning speed in radians per second.
Rotor Tip Speed ($R\omega$)	--	Speed of the blade section at maximum horizontal distance from the axis of rotation.
Rotor Tip Speed Ratio (λ)	--	The ratio of rotor tip speed to the rotor centerline windspeed V_{CL} .
Power Coefficient (C_p)	--	$P_s / A \frac{1}{2} \rho V_{CL}^3$ P_s = rotor shaft power A = rotor area ρ = local APR density V_{CL} = centerline windspeed
Performance Coefficient (K_p)	--	$P_s / A \frac{1}{2} \rho (R\omega)^3 = C_p / \lambda^3$ Usually K_p refers to the maximum value of C_p / λ^3 .
Rated Windspeed	--	A windspeed, at reference height, corresponding to the maximum electrical output of the system.
Cut-Out Windspeed	--	A windspeed at reference height above which the system is shut down.
Cut-In Windspeed	--	The lowest windspeed at reference height for which the system produces positive power.
Annual Energy	--	Total system energy available annually in a specified windspeed distribution.
Rated Power	--	Peak output power produced at rated windspeed. Output power never exceeds this value.
Average Power	--	Total annual energy divided by the number of hours in a year.
Plant Factor	--	Ratio of average to rated power. Indicates the fraction of time the system is at rated power.
Availability or Availability Factor	--	Ratio of annual energy delivered to what is available. Availability factors account for maintenance downtime.

5. Economic Factors

- Annual Charge Rate (ACR) -- The percentage of total system capital costs the user must pay annually to finance the wind energy system.
- Operation and Maintenance (O&M) -- The annual cost required to operate and maintain the system.
- Levelization Factor -- A factor multiplying estimated O&M costs to account for inflation of these costs over the lifetime of the system.

APPENDIX - VERSION 16
ECONOMIC OPTIMIZATION MODEL

- A.1 Definition of Input Data
- A.2 Definition of Output Data
- A.3 Description of Subroutines
- A.4 Complete FORTRAN IV Listing

A.1 Definition of Input Data
(See Fig. A.1 for Typical Input Sequence)

<u>Quantity</u>	<u>Variable Name</u>
Rotor Diameter (ft)	DIA
Number of Blades	BLDS
Height-to-Diameter Ratio	HOD
Struts (see options below)	
Rotor Solidity	XSIG
Blade Wall Thickness-to-Chord Ratio	WALL
Generator Service Factor	SUCG
Transmission Service Factor	SVCT
Line Voltage	VOLTS
Median Windspeed (mph)	VMED
Air Density (lbm/ft ³)	RHO
Wind Shear Exponent	XPON
Rotor Ground Clearance (ft)	HCLR

User Input Options

<u>Option</u>	<u>Means to Select</u>
Blade Struts?	Input 0 for No Struts, 1 for Struts
Optimized or Specified Rotor rpm?	Input Y for Optimized, N for Specified
Rayleigh or Standard Windspeed Distribution?	Input 12, 15, or 18 mph for Standard Distribution. Input Other than 12, 15, or 18 to Obtain Raleigh Distribution.
Change Single Line of Input Used on Previous Run (see Fig. A.2)	Input Line of Input Data to be Changed Following "Changes" Statement
Brief Output?	Input N for Full Output (Fig. A.2); Input Y for Abbreviated Output (The Last Three Lines of Fig. A.2)

ENTER DIAMETER, NUMBER OF BLADES, H/D, STRUTS
 ? 55., 2., 1.5, 0.
 ENTER TURBINE SOLIDITY, BLADE WALL THICKNESS RATIO
 ? .134, .01
 ENTER GEN., TRANS. SERVICE FACTORS, LINE VOLTAGE
 ? 1., 1., 460.
 BRIEF OUTPUT?
 ? N
 WANT OPTIMIZED RPM?
 ? Y
 ENT: MED. W/S, AIR DENS., XPON, HCLR
 ? 15., .076, .17, 7.

Figure A.1 Input Sequence for Version 16

VERS16, 6/30/78, 55.X 83. FT ROTOR 460. VOLTS
 CPK, CPMAX, RE-- .00785 .38598 .16069584E+07
 KMR TIP SPEED RATIOS-- 3.01 5.76 11.47
 PEAK OUTPUTS(KW): ROTOR, TRANS, GEN-- 124.19 119.22 109.70
 PEAK TORQUE, LO SPEED SHAFT-- 16971.9
 RATED WIND SPEED(MPH@ 30'REF)-- 30.96
 TOTAL ENERGY-- 237999. 15.MPH MED. WIND SPEED

CHORD, TURBINE SOLIDITY-- 23.673 .134
 BLADE WALL THICKNESS RATIO, WALL THICKNESS-- .010 .237
 UNSTRUTTED TURBINE, H/D = 1.50
 BLADE GROUND CLEARANCE-- 7.00
 MAX. TORQUE CAPACITY, TRANS-- 16972.
 MAX ELECTRICAL CAPACITY, GEN-- 110.
 TOWER DIA, WALL THICKNESS-- 3.5 .074
 DIAMETER, RPM, TIPSPEED-- 55.00 51.52 148.36
 NET AXIAL LOAD INTO BASE-- 43576.45

ITEM	COST(\$)	PERCENT OF TOTAL	WEIGHT	\$/LB
BLADES	9124.41	17.5	3438.	2.65
TOWER	7232.40	13.9	4822.	1.50
TIEDOWNS	3916.43	7.5	1567.	2.50
TRANS	7893.99	15.2	2037.	3.88
GENERATOR	8993.41	17.3	1359.	6.62
FOUNDATION	2211.99	4.2		
ASSEMBLY	12684.49	24.4		
TOTAL	52057.12	100.0	13222.	3.94
NORMALIZED(\$/KW-HR)--		3.28		
CHANGES OR <CR> TO GO				
?				

Figure A.2 Typical Output Data, Version 16

A.2 Definition of Output Data
(See Fig. A.2 for Typical Output Data)

CPK; CPMAX; RE	--	Maximum Performance Coefficient (K_p , Section 3.1.1); Maximum Power Coefficient; Blade Reynolds Number
K, M, R Tip Speed Ratios	--	Tip Speed Ratios λ_k , λ_m , λ_r Discussed in Section 3.1.1
Peak Outputs (kW), Rotor, Trans, Gen	--	Actual Peak Output Expected at The Rotor, Transmission High Speed Shaft, and Electrical Terminals on the Generator
Peak Torque, Low Speed Shaft	--	Peak Rotor Output Torque, in ft-lbs
Rated Windspeed (mph @ 30' ref.)	--	Windspeed at Which Peak Rotor and System Output Occurs
Total Energy	--	Total Annual Electrical Energy Collection (kWh) in a Given Windspeed Distribution
Chord; Turbine Solidity	--	Blade Chord (inches); Solidity, Defined as the Ratio of Blade Length Times Chord Divided by Rotor Area
Blade Wall Thickness Ratio; Wall Thickness	--	The Ratio of Uniform Wall Thickness to the Blade Chord; Actual Wall Thickness (inches)
Blade Ground Clearance	--	Clearance, in Feet, from the Lower Blade Attachments to Ground Level
Maximum Torque Capacity, Transmission	--	Actual Rating (ft-lbs) of Transmission (May Differ from Peak Rotor Output Torque)
Maximum Electrical Capacity, Generator	--	Actual Rating (kW) of Generator (May Differ from Peak Generator Output)
Tower Diameter; Wall Thickness	--	Tower Outside Diameter (ft); Wall Thickness (in). Dimensions Selected to Meet Structural Requirements
Diameter, rpm, Tip Speed	--	Rotor Diameter (ft); Rotor rpm; Speed of Maximum Radius Portion of Blade (ft/sec)
Net Axial Load into Base	--	Net Force (lbs) at Base of Tower Due to Tiedown Reactions and Total Rotor Weight
Normalized (ϕ /kW-hr)	--	Cost, in <u>Cents</u> per Kilowatt Hour, Calculated by Taking 15% of Total Cost and Dividing by Total Energy
Changes or <CR> To Go?	--	Input Integer to Change Single Line of Input Data. Input Carriage Return <CR> to Repeat Calculation

A.3 Description of Functions and Subroutines in Order
of Their Appearance in Version 16

Functions

POWER(T) -- Calculates electrical power output duration function for integration to determine annual energy. Takes into account the windspeed duration curve, aerodynamic performance of the rotor, and transmission and generator losses.

F(T) -- Windspeed duration function, based on linear interpolation between specified points of velocity and time in hours. Data from F(T) are corrected for wind shear.

CP(TSR) -- Power coefficient as a function of tip speed ratio, using model described in Section 3.1.

POG(PING) -- Output of the generator (kW) as a function of input shaft power PING (kW).

POT(PINT) -- Output of the high speed transmission shaft (kW) as a function of the slow speed shaft input (kW).

Subroutines

PAXIAL -- Calculates the net axial load in the tower. Also calculates required tiedown pretension.

TOWER -- Calculates tower dimensions for minimum volume towers meeting the criteria discussed in Section 3.2.2.

CINSTL -- Calculates foundation and installation costs.

TRANS -- Calculates transmission cost.

GEN -- Calculates generator and electrical controls cost.

CBLADE -- Calculates blade costs.

CPPARM -- Calculates aerodynamic performance parameters for use in function CP(TSR).

LOOK -- A one-dimensional interpolation routine used by CPPARM.

LOOK2D -- A two-dimensional interpolation routine used by CPPARM.

A.4 Complete FORTRAN IV Listing

```

PROGRAM ECON(INPUT,OUTPUT,TAPE4,TAPE66=INPUT,TAPE77=OUTPUT)
COMMON/FV/ND1,VD(200),TD(200)
COMMON/TOWER/TL,HCLR
COMMON/CPTSR/XLK,CPK,XLM,CPMAX,XN,RLRLM
COMMON/ENG/A,PRATED,RW,CON,RLOSSG,RLOSST,S,GR
COMMON/SHEAR/FACT
DIMENSION NND(3),VVD(200,3),TTD(200,3)
DIMENSION Z(50,4,4)
EXTERNAL POWER
CALL INITT(120)
CALL ANMODE
7776 PY=4.*ATAN(1.)
NUM=100
CON1=.96
ICG=0
701 CALL ERASE $ PRINT 720
720 FORMAT(50X/)
IF(ICG.NE.0.AND.ICG.NE.1)GOTO 702
PRINT 101
101 FORMAT(*ENTER DIAMETER,NUMBER OF BLADES,H/D,STRUTS*)
READ *,DIA,BLDS,HOD,STRUT
IF(ICG.NE.0)GOTO 7010
702 IF(ICG.NE.0.AND.ICG.NE.2)GOTO 703
PRINT 104
104 FORMAT(*ENTER TURBINE SOLIDITY,BLADE WALL THICKNESS RATIO*)
READ *,SOL,WALL
IF(ICG.NE.0)GOTO 7010
703 IF(ICG.NE.0.AND.ICG.NE.3)GOTO 704
PRINT 175
175 FORMAT(*ENTER GEN.,TRANS. SERVICE FACTORS,LINE VOLTAGE*)
READ *,SVCG,SVCT,VOLTS
IF(ICG.NE.0)GOTO 7010
704 IF(ICG.NE.0.AND.ICG.NE.4)GOTO 708
PRINT 174
174 FORMAT(*BRIEF OUTPUT+*)
READ 173,IAN$1
IF(ICG.NE.0)GOTO 7010
173 FORMAT(A1)
708 CONTINUE
XFLAG=0.
FLAG=0.
IF(IAN$1.EQ.1HY)FLAG=1.
706 IF(ICG.NE.0.AND.ICG.NE.5)GOTO 707
PRINT 107
107 FORMAT(*WANT OPTIMIZED RPM+*)
READ 173,IAN$
IF(IAN$.EQ.1HY)GO TO 64
PRINT 102
102 FORMAT(*ENTER ROTOR RPM*)
READ *,RPM
XFLAG=1.
64 IF(ICG.NE.0)GOTO 7010
707 CONTINUE
IF(IAN$.NE.1HY)XFLAG=1
F=SQRT(4.+HOD**2)
XLOR=F+.5*HOD*HOD*ALOG((2.+F)/HOD)
1 FORMAT(6F10.3)
ARDEN=.076
IF(ICG.NE.0.AND.ICG.NE.6)GOTO 705
PRINT 60
READ *,VMED,ARDEN,XPON,HCLR
IF(ICG.NE.0)GOTO 7010
705 CONTINUE

```

```

CON=.746*AKDEN/(550.*2.*32.174)
HREF=30.
REWIND 4
DO 50 ITAR=1,3
READ(4,2) ND
NND(ITAB)=ND
DO 6 I=1,ND
READ(4,1) VVD(I,ITAB),TTD(I,ITAB)
5 CONTINUE
50 CONTINUE
2 FORMAT(I10,7F10.0)
103 JTAB = 0
RAY=0.
60 FORMAT(*ENT MED. W/S,AIR DENS.,XPON,HCLR*)
IF(VMED.EQ.12.)JTAB = 1
IF(VMED.EQ.15.)JTAB=2
IF(VMED.EQ.18.)JTAB=3
IF(JTAB.EQ.0)RAY=1.
113 FORMAT(*PRATED,PAVG*,2F10.2)
IF(RAY.EQ.0.)GO TO 246
PRINT 248
248 FORMAT(*ENTER RAYLEIGH AVE WIND SPEED*)
READ *,VMED
CALL RAYDIS(VMED,NUMB,VD,TD)
ND1=NUMB-1
GO TO 900
246 ND=NND(JTAB)
ND1=ND-1
DO 7 I=1,ND
VD(I)=VVD(I,JTAB)
7 TD(I)=TTD(I,JTAB)
900 R=DIA/2.
CALL ERASE
HMIN=12.*DIA*HOD/150.
IF(HCLR.LT.HMIN)HCLR=HMIN
HINCR=HCLR-HMIN
TL=DIA*HOD+HINCR
RW = 80.
IF(XFLAG.EQ.1.)RW=R*RPM*PY/30.
RIN = 10.
OPTMAX = 0.
NI=0
A=8.*R*R*HOD/3.
FACT = ((HOD*R+HCLR)/HREF)**XPON
71 CONTINUE
W = RW/R
S = W*30./PY
C = SOL*12.*A/(RLDS*XLOR*R)
COVR = C/(12.*R)
RE=R*R*W*COVR/1.6197E-4
CALL CPPARM(SOL,HOD,RE,CPK,XLK,CPMAX,XLM,XLR)
XN=3.5
RLKLM=XLK/XLM
RLRLM=XLR/XLM
RPCG=.05
GR=1800./S
RPCT=.04
IF(GR.GT.36.)RPCT=.06
94 SAVE=RPCG
PIR=CON*(RW**3)*CPK*A
PTR=PIR-PIR*RPCT*SVCT
P1=RPCT*SVCT
P2=RPCG*SVCG
PRATED=PIR*(1.-P1-P2+P1*P2)
RPCG=.05*(1000./((PRATED*SVCG)**.215)
ERR=ABS((RPCG-SAVE)/RPCG)

```

```

IF(ERR.GT..05)GO TO 94
RLOSSG=RPCG*PTR*SVCG
RLOSST=RPCT*PIR*SVCT
VIN=60.*RW/(88.*XLR)
VRAT=60.*RW/(88.*XLK)
C
C
C
ERR=.0001
CALL QNC3(POWER,0.,8760.,ERR,E,IERR)
EA = E/A
UTL =E/(8760.*PRATED)
PAVG=E/8760.
TI=PIR*550./(.746*W)
DIA = R*2.
CALL TOWER(R,HOD,XLOR,C,WALL,BLDS,WT1,WT2,WT3,TDIA,TWALL)
CALL CINSTL(CFOUND,CASSEMB,DIA,HOD,HCLR)
PR=PRATED*SVCG
CALL GEN(CGEN,PR,VOLTS)
TR=TI*SVCT
CALL CBLADE(CBLD,BW,BLDS,C,R,NUM,WALL,STRUT,HOD,DUMP)
CALL TRANS(CTRANS,TR)
C
BW=BW*BLDS
TU=WT3+WT2
TLL=BW+WT1+TU
WBSU=14.2E-6*(TU**1.5)
WBSL=14.2E-6*(TLL**1.5)
WST=2.*15.7*(TDIA**3)
WBF=2.*BLDS*.102*C*C*C*169/1728.
WT1=WT1+WBSU+WBSL+WST+WBF
T=BW+WT1+TU
WTRANS=.12*TI*SVCT
WGEN=31.7*PR**.8
WTOT=WGEN+WTRANS+WT1+WT2+BW
CTIE=WT2*2.5
CTOW=WT1*1.5
CBLD=CBLD*BLDS
CT=CBLD+CFOUND+CASSEMB+CTRANS+CGEN+CTOW+CTIE
CNORM=CT*15./E
OPT=1./CNORM
IF(XFLAG.EQ.1.)GO TO 74
IF(OPT.GT.OPTMAX)GO TO 72
NI = NI + 1
IF(NI.EQ.1)GO TO 72
OPTMAX = 0.
IF(NI .GT. 5)GO TO 74
RW = RW - 2.*RIN
RIN = RIN/4.
GO TO 71
72 OPTMAX = OPT
RW = RW + RIN
GO TO 71
74 CONTINUE
IF(FLAG.EQ.1.)GO TO 137
C
DUM=DIA*HOD
PRINT 300,DIA,DUM,VOLTS
300 FORMAT(50X/,3X,*VERS16,6/30/78,*,F4.0,*X*,F4.0,* FT ROTOR*,
1 F6.0,*VOLTS*)
C
PRINT 115,CPK,CPMAX,RE
115 FORMAT(*CPK,CPMAX,RE--,2F10.5,E15.8)
PRINT 116,XLK,XLM,XLR
116 FORMAT(*KMR TIP SPEED RATIOS--,3F10.2)
PRINT 118,PIR,PTR,PRATED

```

```

118 FORMAT(*PEAK OUTPUTS(KW) ROTOR,TRANS,GEN--*,JF8.2)
    PRINT 775, TI
775 FORMAT(*PEAK TORQUE,LO SPEED SHAFT--*,F12.1)
    VRATED=RW*60./(88.*XLK*FACT)
    PRINT 762,VRATED
762 FORMAT(*RATED WIND SPEED(MPH≤ 30+REF)--*,F6.2)
    PRINT 307,E,VMED
307 FORMAT(*TOTAL ENERGY--*,2F10.0,*MPH MED. WIND SPEED*,/)

```

C
C
C
C

```

    PRINT 309,C,SOL
309 FORMAT(*CHORD,TURBINE SOLIDITY--*,2F10.3)
    THICK=WALL*C
    PRINT 330,WALL,THICK
330 FORMAT(*BLADE WALL THICKNESS RATIO,WALL THICKNESS--*,2F10.3)
    IF(STRUT.EQ.1.)PRINT 314,HOD
    IF(STRUT.EQ.0.)PRINT 315,HOD
314 FORMAT(*STRUTTED TURBINE,H/D =*,F4.2)
315 FORMAT(*UNSTRUTTED TURBINE,H/D =*,F4.2)
    PRINT 63,HCLR
    63 FORMAT(*BLADE GROUND CLEARANCE--*,F6.2)
    X=SVCT*TI
576 FORMAT(*MAX. TORQUE CAPACITY,TRANS--*,F10.0)
    PRINT 576,X
    X=PRATED*SVCG
    PRINT 577,X
577 FORMAT(*MAX ELECTRICAL CAPACITY,GEN--*,F10.0)
    PRINT 578,TDIA,TWALL
578 FORMAT(*TOWER DIA,WALL THICKNESS--*,F6.1,F6.3)
    PRINT 310,DIA,S,RW
310 FORMAT(*DIAMETER,RPM,TIPSPEED--*,3F10.2)
    PRINT 313,T
313 FORMAT(*NET AXIAL LOAD INTO BASE--*,F15.2,/)

```

C

```

    PRINT 317
317 FORMAT(*ITEM*,14X,*COST($)*,6X,*PERCENT OF TOTAL*,3X,*WEIGHT*,
15X,*$/LB*)
    W=CBLD*100./CT
    DOL=CBLD/BW
    PRINT 318,CBLD,W,BW,DOL
318 FORMAT(/,*BLADES*,6X,F12.2,10X,F4.1,11X,F8.0,5X,F6.2)
    W=CTOW*100./CT
    DOL=CTOW/WT1
    PRINT 319,CTOW,W,WT1,DOL
319 FORMAT(*TOWER*,7X,F12.2,10X,F4.1,11X,F8.0,5X,F6.2)
    W=CTIE*100./CT
    DOL=CTIE/WT2
    PRINT 320,CTIE,W,WT2,DOL
320 FORMAT(*TIEDOWNS*,4X,F12.2,10X,F4.1,11X,F8.0,5X,F6.2)
    W=CTRANS*100./CT
    DOL=CTRANS/WTRANS
    PRINT 321,CTRANS,W,WTRANS,DOL
321 FORMAT(*TRANS*,7X,F12.2,10X,F4.1,11X,F8.0,5X,F6.2)
    W=CGEN*100./CT
    DOL=CGEN/WGEN
    PRINT 390,CGEN,W,WGEN,DOL
390 FORMAT(*GENERATOR*,3X,F12.2,10X,F4.1,11X,F8.0,5X,F6.2)
    W=CFOUND*100./CT
    PRINT 322,CFOUND,W
322 FORMAT(*FOUNDATION*,2X,F12.2,10X,F4.1)
    W=CASSEMB*100./CT
    PRINT 325,CASSEMB,W
325 FORMAT(*ASSEMBLY*,4X,F12.2,10X,F4.1)
    W=100.

```

```

DOL=CT/WTOT
PRINT 323,CT,W,WTOT,DOL
323 FORMAT(/,*TOTAL*,7X,F12.2,10X,F5.1,11X,F8.0,5X,F6.2)
PRINT 324,CNORM
324 FORMAT(*NORMALIZED($/KW-HR)--*,F10.2)
GO TO 773
137 PRINT 778,PRATED,PAVG,C,CNORM
778 FORMAT(*PRATED,PAVG,C,ORD,$/KW-HR--*,4F10.2)
PRINT 332,S
332 FORMAT(*ROTOR RPM--*,F5.2)
PRINT 323,CT,W,WTOT,DOL
773 CONTINUE
C
C
C
7010 PRINT 667
667 FORMAT(*CHANGES OR <CR> TO GO*)
READ *,ICG
IF(EOF(66))666,665
666 ICG=10
665 IF(ICG.LT.0)STOP
GOTO 701
STOP
END
FUNCTION POWER(T)
COMMON/ENG/A,PRATED,RW,CON,RLOSSG,RLOSST,S,GR
POWER=0.
V=F(T)
IF(V.LE.0.) RETURN
P1 = CON*A*V**3*CP(RW/V)
P2 = POT(P1)
POWER = POG(P2)
RETURN
END
FUNCTION F(T)
COMMON/FV/ND1,VD(200),TD(200)
COMMON/SHEAR/FACT
DO 1 I=1,ND1
J=I
IF(T.GE.TD(I).AND.T.LE.TD(I+1)) GO TO 2
1 CONTINUE
2 F=VD(J)+(VD(J+1)-VD(J))*(T-TD(J))/(TD(J+1)-TD(J))
F=88.*F*FACT/60.
RETURN
END
FUNCTION CP(TSR)
COMMON/CPTSR/XLK,CPK,XLM,CPMAX,XN,RLRLM
IF(TSR.LE.XLK) GO TO 1
IF(TSR.GE.XLM)GO TO 2
A = (TSR-XLM)/(XLK-XLM)
B = CPK*(XLK**3) - CPMAX
CP = CPMAX + A*A*B
RETURN
2 A = (TSR-XLM)/(XLM*RLRLM - XLK)
CP = CPMAX - A*A*CPMAX
RETURN
1 CP=CPK*XLK**3*(TSR/XLK)**XN
RETURN
END
FUNCTION POG(PING)
COMMON/ENG/A,PRATED,RW,CON,RLOSSG,RLOSST,S,GR
CC FUNCTION GIVES OUTPUT GENT POWER AS FUNCTION OF INPUT POWER
C
AA = PRATED**2/(.5*RLOSSG)
B = SQRT(1.+4.*(PING-.5*RLOSSG)/AA)
POG = AA*(B-1.)*.5

```

```

IF (POG .LT. 0.) POG = 0.
RETURN
END
FUNCTION POT (PINT)
COMMON/ENG/A, PRATED, RW, CON, RLOSSG, RLOSST, S, GR
POT = PINT - RLOSST
C
C
C
IF (POT .LE. 0.) POT = 0.
RETURN
END
C
C
SUBROUTINE PAXIAL (R, S, HOD, XLOR, BLDS, C, WALL, WT2, WT3, TOT)
COMMON/TOWER/TL, HCLR
COMMON/PAXIAL/FREQ, AREA, CL, PRET, ATMAX, ATMIN
CC THIS EVALUATES NET AXIAL LOAD ON TOWER
CC DO TIEDOWN PRETENSIONS FIRST
IF (DUMP .NE. 0.) PRINT 71
71 FORMAT (*ENTER PAXIAL*)
PI = 4.*ATAN(1.)
ALFA = 35.*PI/180.
CDEN = 2.07*144./596
EY = 2.9E7
HEIT = HCLR + 2.2*R*HOD
DIST = HEIT/TAN(ALFA)
CL = SQRT(HEIT*HEIT + DIST*DIST)
A = 2.11E-7*CL*CL
E = 3.6E9
DELTA = (4.7E-3*COS(ALFA)*CL*CDEN/E)**(1./3.)
TMIN = CDEN*A*CL*COS(ALFA)/(8.*DELTA)
TMAX = EY*A
TMAX = TMAX/2.
CC EVALUATE TURBINE SIDE LOADS
BL = XLOR*R
F = 410.*C*BL/86.
C THIS IS THE SIDE FORCE AT DESIGN CONDITIONS
FACT = 6./9.
DELT = FACT*F
PRET = DELT + TMIN
ATMAX = PRET + DELT
IF (ATMAX .GT. TMAX) PRET = TMAX - DELT
ATMIN = PRET - DELT
ATMAX = PRET + DELT
X = CDEN*A*CL*COS(ALFA)/(8.*ATMIN)
Y = 512.*E/(12.*COS(ALFA)*CL*CDEN)
SKTAR = X*X*X*Y
DELTA = CDEN*A*CL*COS(ALFA)/(8.*TMIN)
ADENS = 169.
CON = 1.12*(2.*PI/60.)**2/32.2
BAREA = 2.0*C*C*WALL/144.
BD = ADENS*BAREA
TENS = BD*R*R*S*S*CON
CC BLADE TENSION IN LBS
ANG = 59.*PI/180.
IF (HOD .GT. 1.1) ANG = 50.*PI/180.
IF (HOD .GT. 1.3) ANG = 45.*PI/180.
CAX = BLDS*TENS*COS(ANG)
TAX = 3.*PRET*SIN(ALFA)
CPV = A*CL*3.
WT2 = CPV*500.
TOT = CAX + TAX
WT3 = TAX
AREA = A*144.
FREQ = PI*SQRT(PRET*32.2/(CDEN*A))/CL

```

```

      FREQ = FREQ/(2.*PI)
46  RETURN
      END
      SUBROUTINE TOWER(R,HOD,XLOR,C,WALL,BLDS,WT1,WT2,WT3,TDIA,TWALL)
      COMMON/TOWER/TL,HCLR
      ADENS = 169.
      RHOB = 2.0*C*C*ADENS*WALL/(144.*32.2)
      RHO = 500./32.2
      PR = .3
      PI = 4.*ATAN(1.)
      SNEW=200.*60./(R*2.*PI)
      CALL PAXIAL(R,SNEW,HOD,XLOR,BLDS,C,WALL,WT2,WT3,TOT)
      E = 30.E6*144.
      SAVE=TOT
      SFB = 10.
      SFS = 4.
      SMAX = 60000./SFS
      DO = .01*TL
      DINCR = .2*DO
      VMIN=1.E10
      NV = 1
17  N = 1
      DIDOR = .1
      DIDO = 1.
15  CONTINUE
      VOL=PI*DO*DO*(1.-DIDO*DIDO)*TL/4.
      TOT=SAVE+VOL*500./2.+WT2/2.
      PCRITG = PI**3*E*DO**4*(1.-DIDO**4)/(64.*TL*TL)
      PCRITL = PI*E*DO*DO*(1.-DIDO)*(1.-DIDO*DIDO)
      PCRITL = PCRITL/(4.*SQRT(3.*(1.-PR*PR)))
      PJ = BLDS*16.*HOD*RHOB*(R**3)/15.
      G = E/(2.*(1+PR))
      RFREQT = SQRT(G/(PI*TL*PJ))*DO*DO*SQRT(1.-DIDO**4)
      RFREQB = .39*SQRT(E/(RHO*(TL**4)))
      RFREQB = RFREQB*DO*SQRT(1.+DIDO*DIDO)
      PREVT = RFREQT/(SNEW/60.)
      PREVB = RFREQB/(SNEW/60.)
      CRIT = PCRITG/SFB
      IF(TOT.GE.CRIT)GO TO 10
      CRIT = PCRITL/SFB
      IF(TOT.GE.CRIT)GO TO 10
      IF(PREVT.LE.4.)GO TO 10
      IF(DIDO.EQ.1.)DIDO=1.0001
      STRESS = 4.*TOT/(PI*DO*DO*(1.-DIDO*DIDO))
      STRESS = STRESS/144.
      IF(STRESS.GE.SMAX)GO TO 10
      GO TO 16
10  DIDO = DIDO-DIDOR
      IF(DIDO.LT.0.)GO TO 14
      GO TO 15
16  IF(N.GT.5)GO TO 14
      DIDO = DIDO + DIDOR
      DIDOR = DIDOR/5.
      N = N + 1
      GO TO 15
14  CONTINUE
      VOL = PI*DO*DO*(1.-DIDO*DIDO)*TL/4.
      IF(DIDO.LE.0.)GO TO 102
      IF(VOL.GT.VMIN.AND.PREVB.GT.4.)GO TO 6
102 CONTINUE
      VMIN = VOL
      DO = DO + DINCR
      GO TO 17
6  IF(NV.GT.5)GO TO 117
      NV = NV + 1
      VMIN = 1.E10

```

```

DO = DO - DINCR*2.
DINCR = DINCR/5.
GO TO 17
117 CONTINUE
WT1=500.*VOL
TDIA=DO
TWALL=6.*(DO-DIDO*DO)
72 RETURN
END
SUBROUTINE CINSTL(CFOUND,CASSEMB,DIA,HOD,HCLR)
SAVE=DIA
H=DIA*HOD+HCLR
CFOUND=10.6*DIA+.0314*DIA*DIA*(HOD**.66)+.00603*HOD*(DIA**3)
FACT=8.22E-5*HOD*HOD*(H**3.56)
IF(DIA.LT.60.)DIA=60.
IF(FACT.LT.1200.)FACT=1200.
NDAY=3.+DIA*8./60.
FACT2=512.+401.6*((H/60.)**.3)
CASSEMB=1726.+FACT+1186.*((H/60.)**.3)+NDAY*FACT2
IF(SAVE.LT.60.)CASSEMB=1000.+(CASSEMB-1000.)*(SAVE-20.)/40.
IF(SAVE.LT.20.)CASSEMB=1000.
DIA=SAVE
RETURN
END

C
SUBROUTINE TRANS(CTRANS,TI)
CTRANS=3.425*TI**.795
RETURN
END

C
SUBROUTINE GEN(CGEN,PRATED,VOLTS)
CGEN=84.12*(PRATED**.835)
CC COST FORMULA FROM GE CONCEPTUAL DESIGN STUDY
CCON=4000.+18000.*PRATED/375.
CCON1=27000.+7000.*PRATED/1500.
IF(CCON.GT.CCON1)CCON=CCON1
IF(VOLTS.LT.1000.)CCON=2000.+25.*PRATED
CGEN=CGEN+CCON
RETURN
END

C
SUBROUTINE CBLADE(CBLD,TOTW,BLDS,C,R,NUM,WALL,STRUT,HOD,DUMP)
PI=4.*ATAN(1.)
NJOINT=0
TMAXL=60.
TMAXH=12.
NJT=0
STRUTL=0.
RC=.66*R
IF(HOD.GT.1.1)RC=.94*R
IF(HOD.GT.1.3)RC=1.26*R
THETA=112.

C
C
C
IF(HOD.GT.1.1)THETA=98.
IF(HOD.GT.1.3)THETA=89.
ANG=THETA*PI/360.
H=RC*(1.-COS(ANG))
XL=2.*RC*SIN(ANG)
CURVEL=RC*ANG*2.
8 ANG=THETA*PI/(180.*2.*FLOAT(NJOINT+1))
TH=RC*(1.-COS(ANG))
TL=RC*2.*SIN(ANG)
IF(TH.GT.TMAXH)GO TO 10
IF(TL.GT.TMAXL)GO TO 10

```

```

GO TO 99
10 NJOINT=NJOINT+1
GO TO 8
99 CONTINUE
NPEICE=C/24.
NPEICE=NPEICE+1
BWL=0.024*C*C*169./(144.*FLOAT(NPEICE))
CL=RC*2.*ANG
BWL=BWL*WALL/.01
XMAX=5000./BWL
BWL=BWL*FLOAT(NPEICE)
12 IF(XMAX.GT.CL)GO TO 11
CL=CL*FLOAT(NJOINT+1)/FLOAT(NJOINT+2)
NJOINT=NJOINT+1
GO TO 12
11 CONTINUE
NCURVE=NJOINT
SL=.776*R
IF(HOD.GT.1.1)SL=.823*R
IF(HOD.GT.1.3)SL=.858*R
NST=SL/TMAXL
13 TSL=SL/FLOAT(NST+1)
IF(XMAX.GT.TSL)GO TO 14
NST=NST+1
GO TO 13
14 CONTINUE
WTS=TSL*BWL
IF(STRUT.EQ.0.)GO TO 38
STRUTL=.706*R
NJT=STRUTL/TMAXL
37 TSTRUT=STRUTL/FLOAT(NJT+1)
IF(XMAX.GT.TSTRUT)GO TO 38
NJT=NJT+1
GO TO 37
38 CONTINUE
NJOINT=NCURVE+2*NST+2*NJT+2
TOTL=SL*2.+CURVEL+STRUTL*2.
TOTW=TOTL*BWL
CDIE=20000.*FLOAT(NPEICE)/(BLDS*FLOAT(NUM))

```

C
C
C

```

CSETUP=3000.*FLOAT(NPEICE)/(BLDS*FLOAT(NUM))
CMATE=TOTW*2.
CLABJ=12.*2.*TOTL*FLOAT(NPEICE-1)
CLABB=.75*CURVEL*25.
WTJT=BWL*FLOAT(NJOINT)*C*2./12.
CMATJ=WTJT*2.
CBLD=CMATJ+CLABB+CLABJ+CMATE+CSETUP+CDIE
TOTW=TOTW+WTJT
IF(DUMP.EQ.0.)GO TO 15

```

C
C

```

PRINT 16
16 FORMAT(/,* BLADE GEOMETRY RESULTS*)
PRINT 17,CURVEL,H,XL,NCURVE
PRINT 30,C
30 FORMAT(*BLADE CHORD--*,F10.2)
17 FORMAT(/,*CURVED LENGTH,HEIGHT,DRAFT,JOINTS--*,3F10.2,I4)
PRINT 18,SL,NST
18 FORMAT(*STRAIGHT SECTION LENGTH,JOINTS--*,F10.2,I4)
PRINT 19,STRUTL,NJT
19 FORMAT(*STRUT LENGTH, JOINTS--*,F10.2,I4)
PRINT 20,XMAX
20 FORMAT(*MAX EXTRUSION LENGTH--*,F10.2)
PRINT 21,TOTW

```

```

21 FORMAT(*TOTAL BLADE WEIGHT--*,F10.2)
   PRINT 22
22 FORMAT(/,*COST DATA*)
   PRINT 23,CDIE,CSETUP
23 FORMAT(/,*PER BLADE DIE,SETUP COST--*,2F10.2)
   PRINT 24,CLABJ,CLABR
24 FORMAT(*BLADE BONDING,BENDING COSTS--*,2F10.2)
   PRINT 25,CMATE,CMATJ
25 FORMAT(*EXTRUSION MAT COST,JOINT MAT. COST--*,2F10.2)
   PRINT 26,CBLD
26 FORMAT(*TOTAL BLADE COST--*,F10.2)
   CTOTL=CBLD*BLDS
   PRINT 27,CTOTL
27 FORMAT(*TOTAL ROTOR COST--*,F10.2)
15 RETURN
   END

```

C

```

SUBROUTINE CPPARM(SIG,HOD,REC,KPM,XK,CPM,XM,XR)
REAL KPM,LOGREC
DIMENSION AKPM(3,3),BKPM(3,3),AXK(3,3),BXK(3,3),ACPM(3,3),BCPM
1 (3,3),AXM(3,3),BXM(3,3),THOD(3,3),TSIG(3)
COMMON/LIMITS/ILO(4),IHI(4),IR(4),DEN,IEX,VR
DIMENSION Z(4),DZ(4)
DATA (IHI(I),I=1,4)/3,3,3,3/
DATA (ILO(I),I=1,4)/1,1,1,1/
DATA (IR(I),I=1,4)/1,1,1,1/
DATA (THOD(I),I=1,9)/1.0,1.25,1.5,1.0,1.25,1.5,1.0,1.25,1.5/
DATA (TSIG(I),I=1,3)/0.05,0.132,0.20/

```

C

```

NACA 0015
DATA (AKPM(I),I=1,9)/-2.393,-7.183,-3.378,-5.319,-7.295,-9.057,
1 -11.649,-22.539,-14.359/
DATA (BKPM(I),I=1,9)/0.360,0.667,0.443,0.882,1.039,1.166,
1 1.571,2.285,1.785/
DATA (AXK(I),I=1,9)/3.631,7.217,3.748,3.480,4.235,4.285,
1 3.726,4.328,4.497/
DATA (BXK(I),I=1,9)/-0.030,-0.242,-0.034,-0.034,-0.083,-0.088,
1 -0.060,-0.101,-0.110/
DATA (ACPM(I),I=1,9)/0.213,0.099,0.238,0.350,0.334,0.328,
1 0.345,0.336,0.340/
DATA (BCPM(I),I=1,9)/0.001,0.012,0.003,0.001,0.003,0.004,
1 0.003,0.004,0.004/
DATA (AXM(I),I=1,9)/4.662,6.740,4.871,6.204,7.023,7.695,
1 4.909,3.935,1.214/
DATA (BXM(I),I=1,9)/0.281,0.163,0.268,0.013,-0.075,-0.131,
1 -0.007,0.042,0.211/
LOGREC=ALOG(REC)
CALL LOOK2D(4,SIG,TSIG,0,HOD,THOD,AKPM,BKPM,AXK,BXK,Z,DZ,4,3)
KPM = Z(1) + Z(2)*LOGREC
KPM=KPM*.001
XK = Z(3) + Z(4)*LOGREC
CALL LOOK2D(4,SIG,TSIG,0,HOD,THOD,ACPM,BCPM,AXM,BXM,Z,DZ,4,3)
1000 FORMAT(10X,4(2XF7.3))
CPM = Z(1) + Z(2)*LOGREC
XM = Z(3) + Z(4)*LOGREC
XR = 1.04*LOGREC - 3.45*ALOG(SIG) - 10.45
RETURN
END

```

C

```

SUBROUTINE LOOK (II,XL,X,A,B,C,E,Y,D,IDN)
COMMON/LIMITS/ILO(4),IHI(4),IR(4),DEN,IEX,VR
DIMENSION X(1), A(1), B(1), C(1), E(1), Y(1), D(1)
IH=IHI(II)
IL=ILO(II)
DO 5 J=1,IDN
D(J) = 0.0
Y(J) = 0.0

```

```

5 CONTINUE
  VR = 0.0
  IEX=0
  IF (X(IH)-X(IL)) 10,10,30
10  IEX=1
  IF (XL-X(IH)) 120,130,20
20  IF (XL-X(IL)) 50,150,140
30  IF (XL-X(IH)) 40,130,120
40  IF (XL-X(IL)) 140,150,50
50  I=IR(II)
  I=MIN0(I,IH)
  I=MAX0(I,IL)
  IS=1
  IT=1
  GO TO 70
60  I=I+1
  IS=0
70  IF (IEX) 80,80,90
80  IF (XL-X(I)) 100,160,110
90  IF (XL-X(I)) 110,160,100
100 I=I-1
  IT=0
  IF (IS) 160,160,70
110 IF (IT) 160,160,60
120 IEX=3
130 I=IH-1
  GO TO 160
140 IEX=2
150 I=IL
160 DEN=X(I+1)-X(I)
  IR(II)=I
  VR=XL-X(I)
  IF (IDN) 230,230,170
170 GO TO (210,200,190,180), IDN
180 Y(4)=E(I)
  D(4)=E(I+1)-E(I)
190 Y(3)=C(I)
  D(3)=C(I+1)-C(I)
200 Y(2)=B(I)
  D(2)=B(I+1)-B(I)
210 Y(1)=A(I)
  D(1)=A(I+1)-A(I)
  IF (DEN.EQ.0.0) RETURN
  DO 220 J=1, IDN
  D(J)=D(J)/DEN
220 Y(J)=Y(J)+D(J)*VR
230 VR=VR/DEN
  RETURN
  END

```

C

```

SUBROUTINE LOOK2D(II,XL,X,IF,YL,Y,A,B,C,E,Z,DZ,NLOOK,ND)
COMMON/LIMITS/ILO(4),IHI(4),IR(4),DEN,IEX,VR
DIMENSION X(1), Y(ND,1), A(ND,1), B(ND,1), C(ND,1),
1 E(ND,1), Z(4), DZ(4), ZL(4), DZL(4), ZR(4),
2 DZR(4)
  VRS = 1.0
  J = 0
  DO 10 I=1,NLOOK
  Z(I) = DZ(I) = 0.0
10 CONTINUE
  IF (IHI(II).EQ.1) GO TO 20
  CALL LOOK(II,XL,X,0,0,0,0,Z,DZ,0)
  VRS = VR
  J = IR(II)
  JJ = IF + J
  CALL LOOK(JJ,YL,Y(1,J),A(1,J),B(1,J),C(1,J),E(1,J),Z,DZ,NLOOK)

```

```

DO 15 I=1,NLOOK
ZL(I) = Z(I)
DZL(I) = DZ(I)
15 CONTINUE
20 CONTINUE
J = J + 1
JJ = IF + J
CALL LOOK(JJ,YL,Y(1,J),A(1,J),B(1,J),C(1,J),E(1,J),Z,DZ,NLOOK)
DO 30 I=1,NLOOK
ZR(I) = Z(I)
DZR(I) = DZ(I)
30 CONTINUE
VRSP = 1. - VRS
DO 40 I=1,NLOOK
Z(I) = ZL(I)*VRSP + ZR(I)*VRS
DZ(I) = DZL(I)*VRSP + DZR(I)*VRS
40 CONTINUE
RETURN
END
SUBROUTINE RAYDIS(XMEAN,NUMB,VEL,HOURS)
DIMENSION VEL(1),HOURS(1)
C COMPUTES A RAYLEIGH DISTRIBUTION WITH A PRESCRIBED MEAN
RAY(X,RC2,RC22)=(X*RC2)*EXP(-X*X*RC22)
C=XMEAN/1.2533
C2=C*C
RC2=1./C2
RC22=RC2/2.
C
C FIND UPPER LIMIT FOR OPERATION
C
X=25.
1 Y=RAY(X,RC2,RC22)
IF(Y.LT.1.E-5)GO TO 5
X=X+1.
GO TO 1
5 YTOT=0.
NUMB=X+1.
DO 10 J=1,NUMB
X=FLOAT(NUMB-J+1)
Y=RAY(X,RC2,RC22)
VEL(J)=X
HOURS(J)=YTOT*8760.
10 YTOT=Y+YTOT
RETURN
END

```

DISTRIBUTION:

TID-4500-R66 UC-60 (283)

Aero Engineering Department (2)
Wichita State University
Wichita, KS 67208
Attn: M. Snyder
W. Wentz

Dr. Daniel K. Ai
Senior Scientific Associate
Alcoa Laboratories
Aluminum Company of America
Alcoa Center, PA 15069

R. E. Akins, Assistant Professor
Department of Engineering Science
and Mechanics
Virginia Polytechnic Institute and
State University
Blacksburg, VA 24060

Mr. Robert B. Allen
General Manager
Dynergy Corporation
P.O. Box 428
1269 Union Avenue
Laconia, NH 03246

American Wind Energy Association
54468 CR31
Bristol, IN 46507

E. E. Anderson
South Dakota School of Mines
and Technology
Department of Mechanical Engineering
Rapid City, SD 57701

Scott Anderson
318 Millis Hall
University of Vermont
Burlington, VT 05405

George W. Barnes
Barnes Engineering Co.
1645 South Claudina Way
Anaheim, CA 92805

F. K. Bechtel
Washington State University
Department of Electrical Engineering
College of Engineering
Pullman, WA 99163

M. E. Beecher
Arizona State University
Solar Energy Collection
University Library
Tempe, AZ 85281

K. Bergey
University of Oklahoma
Aero Engineering Department
Norman, OK 73069

Dr. B. F. Blackwell
Department of Mechanical Engineering
Louisiana Tech University
Ruston, LA 71270

Steve Blake
Wind Energy Systems
Route 1, Box 93-A
Oskaloosa, KS 66066

Robert Brulle
McDonnell-Douglas
P.O. Box 516
Department 241, Building 32
St. Louis, MO 63166

R. Camerero
Faculty of Applied Science
University of Sherbrooke
Sherbrooke, Quebec
CANADA J1K 2R1

Professor V. A. L. Chasteau
School of Engineering
University of Auckland
Private Bag
Auckland, NEW ZEALAND

Howard T. Clark
McDonnell Aircraft Corporation
P.O. Box 516
Department 337, Building 32
St. Louis, MO 63166

Dr. R. N. Clark
USDA, Agricultural Research Service
Southwest Great Plains Research Center
Bushland, TX 79012

Arthur G. Craig
Alcoa Mill Products
Alcoa Center, PA 15069

Dr. D. E. Cromack
Associate Professor
Mechanical and Aerospace Engineering
Department
University of Massachusetts
Amherst, MA 01003

DOE/ALO (3)
Albuquerque, NM 87185
Attn: D. K. Nowlin
W. P. Grace
D. W. King

DOE Headquarters (20)
Washington, DC 20545
Attn: L. V. Divone, Chief
Wind Systems Branch
G. T. Tennyson, Program Manager
Wind Systems Branch
D. F. Ancona, Program Manager
Wind Systems Branch

C. W. Dodd
School of Engineering
Southern Illinois University
Carbondale, IL 62901

D. P. Dougan
Hamilton Standard
1730 NASA Boulevard
Room 207
Houston, TX 77058

J. B. Dragt
Netherlands Energy Research Foundation (E.C.N.)
Physics Department
Westerduinweg 3 Patten (nh)
THE NETHERLANDS

C. E. Elderkin
Battelle-Pacific Northwest Laboratory
P.O. Box 999
Richland, WA 99352

Frank R. Eldridge, Jr.
The Mitre Corporation
1820 Dolley Madison Blvd.
McLean, VA 22102

Electric Power Research Institute
3412 Hillview Avenue
Palo Alto, CA 94304
Attn: E. Demeo

James D. Fock, Jr.
Department of Aerospace Engineering Sciences
University of Colorado
Boulder, CO 80309

Albert Fritzsche
Dornier System GmbH
Postfach 1360
7990 Friedrichshafen
WEST GERMANY

W. W. Garth, IV
Tyler & Reynolds & Craig
One Boston Place
Boston, MA

E. Gilmore
Amarillo College
Amarillo, TX 79100

Roger T. Griffiths
University College of Swansea
Department of Mechanical Engineering
Singleton Park
Swansea SA2 8PP
UNITED KINGDOM

Professor N. D. Ham
Massachusetts Institute of Technology
77 Massachusetts Avenue
Cambridge, MA 02139

Sam Hansen
DOE/DST
20 Massachusetts Avenue
Washington, DC 20545

W. L. Harris
Aero/Astro Deptment
Massachusetts Institute of Technology
Cambridge, MA 02139

Terry Healy (2)
Rocky Flats Plant
P.O. Box 464
Golden, CO 80401

Helion
P.O. Box 4301
Sylmar, CA 91342

Don Hinrichsen
Associate Editor
AMBIO
KVA
Fack, S-10405
Stockholm
SWEDEN

J. T. Huang
Alcoa Laboratories
Aluminum Company of America
Alcoa Center, PA 15069

Sven Hugosson
Box 21048
S. 100 31 Stockholm 21
SWEDEN

O. Igra
Department of Mechanical Engineering
Ben-Gurion University of the Negev
Beer-Sheva, ISRAEL

JBF Scientific Corporation
2 Jewel Drive
Wilmington, MA 01887
Attn: E. E. Johanson

Dr. Gary L. Johnson, P.E.
Electrical Engineering Department
Kansas State University
Manhattan, KS 66506

J. P. Johnston
Stanford University
Department of Mechanical Engineering
Stanford, CA 94305

J. R. Jombock
Alcoa Laboratories
Aluminum Company of America
Alcoa Center, PA 15069

Kaman Aerospace Corporation
Old Windsor Road
Bloomfield, CT 06002
Attn: W. Batesol

Robert E. Kelland
The College of Trades and Technology
P.O. Box 1693
Prince Philip Drive
St. John's, NEWFOUNDLAND
A1C 5P7

Larry Kinnett
P.O. Box 6593
Santa Barbara, CA 93111

O. Krauss
Michigan State University
Division of Engineering Research
East Lansing, MI 48824

Lawrence Livermore Laboratory
P.O. Box 808 L-340
Livermore, CA 94550
Attn: D. W. Dorn

M. Lechner
Public Service Company of New Mexico
P.O. Box 2267
Albuquerque, NM 87103

George E. Lennox
Industry Director
Mill Products Division
Reynolds Metals Company
6601 West Broad Street
Richmond, VA 23261

J. Lerner
State Energy Commission
Research and Development Division
1111 Howe Avenue
Sacramento, CA 95825

L. Liljidahl
Building 303
Agriculture Research Center
USDA
Beltsville, MD 20705

P. B. S. Lissaman
Aeroenvironment, Inc.
660 South Arroyo Parkway
Pasadena, CA 91105

Olle Ljungstrom
FFA, The Aeronautical Research Institute
Box 11021
S-16111 Bromma
SWEDEN

Los Alamos Scientific Laboratories
P.O. Box 1663
Los Alamos, NM 87544
Attn: J. D. Balcomb Q-DO-T
Library

Ernel L. Luther
Senior Associate
PRC Energy Analysis Co.
7600 Old Springhouse Rd.
McLean, VA 22101

L. H. J. Maile
48 York Mills Rd.
Willowdale, Ontario
CANADA M2P 1B4

Frank Matanzo
Dardalen Associates
15110 Frederick Road
Woodbine, MD 21797

J. R. McConnell
Tumac Industries, Inc.
650 Ford St.
Colorado Springs, CO 80915

James Meiggs
Kaman Sciences Corporation
P.O. Box 7463
Colorado Springs, CO 80933

R. N. Meroney
Colorado State University
Department of Civil Engineering
Fort Collins, CO 80521

G. N. Monsson
Department of Economic Planning
and Development
Barrett Building
Cheyenne, WY 82002

NASA
Langley Research Center
Hampton, VA 23665
Attn: R. Muraca, MS317

NASA Lewis Research Center (2)
2100 Brookpark Road
Cleveland, OH 44135
Attn: J. Savino, MS 509-201
R. L. Thomas
W. Robbins
K. Kaza, MS 49-6

V. Nelson
West Texas State University
Department of Physics
P.O. Box 248
Canyon, TX 79016

Leander Nichols
Natural Power, Inc.
New Boston, NH 03070

Oklahoma State University (2)
Stillwater, OK 76074
Attn: W. L. Hughes
EE Department
D. K. McLaughlin
ME Department

Oregon State University (2)
Corvallis, OR 97331
Attn: R. Wilson
ME Department
R. W. Thresher
ME Department

H. H. Paalman
Dow Chemical USA
Research Center
2800 Mitchell Drive
Walnut Creek, CA 94598

R. A. Parmelee
Northwestern University
Department of Civil Engineering
Evanston, IL 60201

Art Parthe
Draper Laboratory
555 Technology Square
Mail Station 22
Cambridge, MA 02139

Helge Petersen
Riso National Laboratory
DK-4000 Roskilde
DENMARK

Dr. Barry Rawlings, Chief
Division of Mechanical Engineering
Commonwealth Scientific and Industrial
Research Organization
Graham Road, Highett
Victoria, 3190
AUSTRALIA

Thomas W. Reddoch
Associate Professor
Department of Electrical Engineering
The University of Tennessee
Knoxville, TN 37916

A. Robb
Memorial University of Newfoundland
Faculty of Engineering and Applied Sciences
St. John's Newfoundland
CANADA A1C 5S7

Dr. L. Schienbein
Development Engineer
DAFINDAL Limited
3570 Hawkestone Rd.
Mississauga, Ontario
CANADA L5C 2V8

Arnan Seginer
Professor of Aerodynamics
Technion-Israel Institute of
Technology
Department of Aeronautical
Engineering
Haifa, ISRAEL

Dr. Horst Selzer
Dipl.-Phys.
Wehrtechnik und Energieforschung
ERNO-Raumfahrttechnik GmbH
Hunefeldstr. 1-5
Postfach 10 59 09
2800 Bremen 1
GERMANY

H. Sevier
Rocket and Space Division
Bristol Aerospace Ltd.
P.O. Box 874
Winnipeg, Manitoba
CANADA R3C 2S4

P. N. Shankar
Aerodynamics Division
National Aeronautical Laboratory
Bangalore 560017
INDIA

David Sharpe
Kingston Polytechnic
Canbury Park Road
Kingston, Surrey
UNITED KINGDOM

D. G. Shepherd
Cornell University
Sibley School of Mechanical and
Aerospace Engineering
Ithaca, NY 14853

Dr. Fred Smith
Mechanical Engineering Department Head
Colorado State University
Ft. Collins, CO 80521

Leo H. Soderholm
Iowa State University
Agricultural Engineering, Room 213
Ames, IA 50010

Howard Sonksen
18600 Main St.
Huntington Beach, CA 92648

Southwest Research Institute (2)
P.O. Drawer 28501
San Antonio, TX 78284
Attn: W. L. Donaldson, Senior Vice President
R. K. Swanson

Rick Stevenson
Rt. 10
Box 830
Springfield, MO 65803

Dale T. Stjernholm, P.E.
Mechanical Design Engineer
Morey/Stjernholm and Associates
1050 Magnolia Street
Colorado Springs, CO 80907

R. J. Templin (3)
Low Speed Aerodynamics Section
NRC-National Aeronautical Establishment
Ottawa 7, Ontario
CANADA K1A 0R6

Texas Tech University (3)
P.O. Box 4289
Lubbock, TX 79409
Attn: K. C. Mehta, CE Department
J. Strickland, ME Department
J. Lawrence, ME Department

Fred Thompson
Atari, Inc.
155 Moffett Park Drive
Sunnyvale, CA 94086

United Engineers and Constructors, Inc.
Advanced Engineering Department
30 South 17th Street
Philadelphia, PA 19101
Attn: A. J. Karalis

United Nations Environment Program
485 Lexington Avenue
New York, NY 10017
Attn: I. H. Usmani

University of New Mexico (2)
Albuquerque, NM 87106
Attn: K. T. Feldman
Energy Research Center
V. Sloglund
ME Department

Irwin E. Vas
Solar Energy Research Institute
1536 Cole Blvd.
Golden, CO 80401

P. N. Vosburgh, Development Manager
Alcoa Allied Products
Aluminum Company of America
Alcoa Center, PA 15069

Otto de Vries
National Aerospace Laboratory
Anthony Fokkerweg 2
Amsterdam 1017
THE NETHERLANDS

R. Walters
West Virginia University
Department of Aero Engineering
1062 Kountz Avenue
Morgantown, WV 26505

E. J. Warchol
Bonneville Power Administration
P.O. Box 3621
Portland, OR 97225

D. F. Warne, Manager
Energy and Power Systems
ERA Ltd.
Cleeve Rd.
Leatherhead
Surrey KT22 7SA
ENGLAND

R. J. Watson
Watson Bowman Associates, Inc.
1280 Niagara St.
Buffalo, NY 14213

R. G. Watts
Tulane University
Department of Mechanical Engineering
New Orleans, LA 70018

Pat Weis
Solar Energy Research Institute
1536 Cole Blvd.
Golden, CO 80401

W. G. Wells, P.E.
Associate Professor
Mechanical Engineering Department
Mississippi State University
Mississippi State, MS 39762

T. Wentink, Jr.
University of Alaska
Geophysical Institute
Fairbanks, AK 99701

West Texas State University
Government Depository Library
Number 613
Canyon, TX 79015

Wind Energy Report
Box 14
104 S. Village Ave.
Rockville Centre, NY 11571
Attn: Farrell Smith Seiler

C. Wood
Dominion Aluminum Fabricating Ltd.
3570 Hawkestone Road
Mississauga, Ontario
CANADA L5C 2V8

1000 G. A. Fowler
1200 L. D. Smith
3141 T. L. Werner (5)
3151 W. L. Garner (3)
For DOE/TIC (Unlimited Release)
3161 J. E. Mitchell (15)
3161 P. S. Wilson
4533 J. W. Reed
4700 J. H. Scott
4710 G. E. Brandvold
4715 R. H. Braasch (100)
4715 R. D. Grover
4715 E. G. Kadlec
4715 R. O. Nellums
4715 W. N. Sullivan
4715 M. H. Worstell
5520 T. B. Lane
5521 D. W. Lobitz
5523 R. C. Reuter, Jr.
5523 T. G. Carne
5523 P. J. Sutherland
5600 D. B. Schuster
5620 M. M. Newsom
5630 R. C. Maydew
5632 C. W. Peterson
5632 P. C. Klimas
5633 S. McAlees, Jr.
5633 R. E. Sheldahl
8266 E. A. Aas
DOE/TIC (25)
(R. P. Campbell, 3172-3)

